

URANIUM CONTAMINATION OF VADOSE ZONE SEDIMENTS FROM  
THE HANFORD U SINGLE SHELL TANK FARM

By

BENJAMIN DEETER WILLIAMS

A thesis submitted in partial fulfillment of  
the requirements for the degree of

MASTER OF SCIENCE IN ENVIRONMENTAL SCIENCE

WASHINGTON STATE UNIVERSITY  
School of Earth and Environmental Sciences

DECEMBER 2009


To the Faculty of Washington State University:

The members of the Committee appointed to examine the thesis of  
BENJAMIN DEETER WILLIAMS find it satisfactory and recommend that it be accepted.



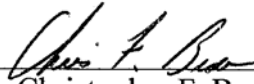
---

Akram Hoossain, Ph.D., Chair



---

Wooyong Um, Ph.D.



---

Christopher F. Brown, M.S.

# URANIUM CONTAMINATION OF VADOSE ZONE SEDIMENTS FROM THE HANFORD U SINGLE SHELL TANK FARM

## Abstract

By Benjamin Deeter Williams, M.S.  
Washington State University  
December 2009

Chair: Akram Hossain

Direct push core samples were collected from direct-push hole C5602 near waste storage tank 241-U-105 in Hanford's 241-U Single-Shell Tank Farm. Uranium concentrations decreased with depth in sediments collected from the direct-push hole. Initial characterization testing revealed that uranium from intermediate depth sediments had lower desorption  $K_{ds}$  than the other sediments. Subsequent investigations on these sediments suggested that uranium existed as different surface phases on the sediments as a function of depth (Um et al. 2009). Further work was carried out to elucidate the nature of U(VI) release from these contaminated sediments. Of particular interest was the observation that the shallow sediments, which were thought to contain contaminant uranium in the form of U(VI) silicates, seem to have similar  $K_{ds}$  to that of the deepest sediment collected from the direct-push hole, which were thought to contain only natural uranium. The primary objective of this research was to determine if the dominant form of uranium in the shallowest sediments collected from direct-push hole C5602 differ from the deeper samples, and if it could be confirmed that uranium in the shallowest sediment was present primarily as U(VI) silicates.

Table of Contents	Page
Abstract .....	iii
1.0 Introduction .....	1
2.0 Materials and Methods .....	4
2.1. Sediment Collection.....	4
2.2. Uranium Adsorption Batch Reaction.....	5
2.3. Uranium Leaching Batch Reaction.....	6
2.3.1.(Bi)carbonate Leaching.....	7
2.3.2.Synthetic Ground Water With Elevated Na & Si Leaching .....	7
2.4. X-Ray Diffraction .....	8
3.0 Results and Discussion.....	8
3.1. Sediment Characterization.....	8
3.2. Uranium Adsorption Batch Reaction.....	10
3.3. Uranium Leaching Batch Reaction.....	14
3.3.1.De-ionized Water Leaching .....	15
3.3.2.(Bi)carbonate Leaching.....	16
3.3.3.SGW Leaching.....	17
3.3.4.SGW+Na <sub>2</sub> SiO <sub>3</sub> Leaching.....	18
4.0 Conclusions .....	19
Acknowledgment .....	23

Table of Contents - continued.....	Page
Appendix.....	24
References.....	49
Figure Captions.....	52
Table Captions .....	53

Uranium contamination of vadose zone sediments from the Hanford U single shell tank farm.

Benjamin D. Williams\*

*Pacific Northwest National Laboratory, Richland, WA 99352*

For Submission to: *Applied Geochemistry*

\* Corresponding Author: Pacific Northwest National Laboratory, P.O. Box 999, MSIN P7-22, Richland, Washington 99352; Phone: (509) 376-1655; Fax: (509) 376-4890; E-Mail Address: benjamin.williams@pnl.gov.

## 1.0 Introduction

Among the first waste storage tanks built at the Hanford Site near Richland, WA were those of the U tank farm. They held a variety of radioactive wastes from different operational processes that occurred over nearly 45 years. Since that time, remediation of soil and groundwater contamination and protection of the Columbia River have been paramount objectives at the Hanford Site. Uranium is a common contaminant in the Hanford environment. In near-surface oxidizing environments, such as the vadose zone at the Hanford Site, U(VI) is prevalent over U(IV) and exists primarily as the uranyl ion ( $\text{UO}_2^{2+}$ ) below pH 5, or the hydroxyl complexes [ $\text{UO}_2\text{OH}^+$ ,  $\text{UO}_2(\text{OH})_2$ ,  $\text{UO}_2(\text{OH})_3^-$ ,  $(\text{UO}_2)_3(\text{OH})_5^+$ ,  $(\text{UO}_2)_2(\text{OH})_2^{2+}$ ] it forms at higher pH conditions (Finch and Murakami, 1999; Jenne, 1998; Langmiur, 1997). As pH increases from 3.5 to 8, uranium adsorption also tends to increase due to the increased number of sorption sites. Of particular significance with regard to the Hanford Site are the uranyl carbonate complexes [ $(\text{UO}_2)_2\text{CO}_3(\text{OH})_3^-$ ,  $\text{UO}_2(\text{CO}_3)_2^{2-}$ ,  $\text{UO}_2(\text{CO}_3)_3^{4-}$ ] which begin to dominate uranium sediment-water chemistry above pH 6.5 and form strong complexes that promote U(IV) oxidation to U(VI) and U mineral dissolution while inhibiting uranium sorption (Dong, et al., 2005; Grenthe, et al., 1992; Mason, et al., 1997; Zachara, et al., 2007a). This leads to increased uranium mobility through sediments (Finch and Murakami, 1999; Gadelle, et al., 2001; Kohler, et al., 2004; Zachara, et al., 2007b). Dissolved silica is also a common component of natural groundwater (Drever, 2002; Jenne, 1998; Snoeyink and Jenkins, 1980).

Oxidation of uranium in uranium mine tailings and spent nuclear fuel, may lead to formation of secondary uranium bearing minerals. In the Hanford environment where Ca and Si are also present, uranophane ( $\text{Ca}(\text{UO}_2)_2(\text{SiO}_3\text{OH})_2 \cdot 5\text{H}_2\text{O}$ ) may be a common secondary

mineral. Further alteration may lead to the formation of boltwoodite ( $K_2(UO_2)_2(SiO_3)_2(OH)_2 \cdot 3H_2O$ ) and other alteration products. Both uranophane and boltwoodite have been found to exist in other Hanford sediments (Ilton, et al., 2008; McKinley, et al., 2007). In groundwater of circum-neutral to alkaline pH where secondary uranium minerals have low solubility, uranium may precipitate as a uranyl silicate mineral, such as boltwoodite or uranophane, where dissolved calcium is also present.

Historically, U farm tank wastes have contained an average of  $2.52 \times 10^5$   $\mu\text{g/L}$  uranium (Hodges and Chou, 2000b). Uranium bearing tank wastes are commonly at pH 10.5 or greater, partly due to over neutralization in order to minimize tank corrosion (Kaplan, et al., 1998). High temperatures, in the range of 70-100° F, are also common due to the continuously reactive nature of the waste cocktail in the tanks (Brevick, et al., 1997). When these hot, alkaline uranium bearing wastes contact the Hanford sediments, the liquid waste reacts with the sediment resulting in near-field U-containing precipitates (Catalano, et al., 2006; Singer, et al., 2009), possibly uranyl silicates (Ilton, et al., 2008; McKinley, et al., 2007; Qafoku, et al., 2005). Furthermore, uranium adsorption may occur at more remote locations where the sediment buffering capacity has not been exceeded by the free hydroxide in the alkaline tank waste, resulting in lower pH conditions. The sorbed uranium and uranium solid phases are thought to be potential secondary sources for long-term U(VI) release from contaminated sediments to pore water and groundwater (Arai, et al., 2007; McKinley, et al., 2007; Wellman, et al., 2008). Prediction and management of uranium migration and potential movement to groundwater and the Columbia River is heavily influenced by the nature of uranium in the sediments and depends on its source as a sorbed surface complex or mineral precipitate.



As part of an ongoing soil contamination characterization and remediation effort, sediment samples were collected from direct-push hole C5602, which was emplaced a few feet southeast of tank 241-U-105 at the U tank farm (Figure 1). This location is in an area encompassed by potential contamination from several sources (Crumpler, 2004; Field and Jones, 2005; Wood and Jones, 2003) and resulted in a vadose zone uranium contaminant plume about 100 feet wide extending approximately 225 feet toward the southwest (Figure 2). Consequent to the release of multiple waste streams with varying chemical compositions to U farm sediments, multiple forms of uranium are anticipated to exist in the underlying contaminated sediments.

Based on previous sediment characterization (Brown, et al., 2007), uranium concentrations were found to generally decrease with depth, with the deepest samples containing what is probably natural background uranium. Initial characterization results also indicated that uranium from the shallowest and deepest sediments had higher equilibrium desorption  $K_d$ s than did intermediate depth sediments. The relatively low uranium  $K_d$  found in the shallow, highly contaminated sediments seemed anomalous and implied some similarity in the nature of the uranium contained in these two depth zones. Batch (bi)carbonate leaching tests suggested two release mechanisms, initial rapid U desorption followed by dissolution of uranium bearing precipitates (Um, et al., 2009). Subsequent macroscopic and spectroscopic investigations (XAFS, XRF and TRLIF) on these sediments indicated that U(VI) existed as different surface phases on the vadose zone sediments as a function of depth (Um, et al., 2009). Based on these analyses, uranium contamination found in the shallow sediments U(VI) seemed to be predominantly in the form of U(VI) silicate precipitates, such as boltwoodite and uranophane, which have been found to exist in other Hanford sediments (Ilton, et al., 2008; McKinley, et al., 2007).

Although these secondary mineral precipitates were thought to be present, it was not known how or if they contributed to short and/or long term release of uranium. The objective of this current study was to show that uranium mobility characteristics vary with depth and to confirm the presence of uranyl silicate precipitates in the shallowest sediment, H0A-52.3. With the exception of the deep background samples, all sediments from direct-push hole C5602 contain elevated levels of uranium. The goal was to determine which uranium release mechanism was involved with the hope that it might also shed light on the nature of uranium uptake by the sediments. Motivated by the observation that shallow and deep sediments from this direct-push hole had similar  $K_d$  estimates, yet distinctly higher  $K_d$ s than intermediate sediments, and the desire to understand this apparent paradox, the primary objective was to confirm the presence of uranium silicate mineral precipitates in sediment H0A-52.3 and to illustrate its dominance as a driver of long-term uranium release to the vadose zone and groundwater.

## **2.0 Materials and Methods**

### **2.1. Sediment Collection**

Sediment samples (Table 1) were collected using the direct push method in which a casing is progressively driven into surface sediments and samples are retrieved as sleeved cores (Byrnes, 2001). Sample intervals were encompassed by vertically contiguous but discrete core sleeves that were sealed on arrival at the surface. Because contaminant uranium concentrations tend to be higher with regard to the smaller particle-size fractions of Hanford sediments, samples

were sieved in order to remove particle sizes greater than 2mm (Cantrell, et al., 2003; Last, et al., 2006).

## **2.2. Uranium Adsorption Batch Reaction**

Prior characterization (Brown, et al., 2007) had identified the deepest sample, B1PBB0A (92.3' bgs), as having had little to no contact with a man-made uranium-bearing liquid waste stream. Consequently, this sample was selected for a batch reaction designed to yield an adsorption isotherm that might be applied to all of the sediments from direct-push hole C5602.

The batch reaction was performed using a synthetic groundwater (SGW), composition shown in Table 2, similar to others that have been used in previous Hanford investigations (Ilton, et al., 2008; Liu, et al., 2008; Qafoku, et al., 2005). The SGW was equilibrated with excess  $\text{CaCO}_3$  for a minimum of one week in order to simulate Hanford groundwaters in equilibrium with calcite (Deutsch, et al., 2007; Liu, et al., 2004; Wellman, et al., 2008; Zachara, et al., 2007b). Following equilibration and prior to use in the batch reaction, the SGW was filtered to 0.45 microns in order to remove potential excess  $\text{CaCO}_3$  precipitate.

Sample B1PBB0A was prepared for the adsorption batch reaction by oven drying at 45° C for 3 days. Three gram aliquots of B1PBB0A were measured into each of ten 50ml centrifuge tubes. Each aliquot was gently pre-washed with 30ml of SGW for 24 hours on a mechanical shaker in order to equilibrate the sediment with the solution. After 24 hours of washing, the tubes were centrifuged for 4 minutes at 3000 rpm in a Thermo Electron Corp. HN SII centrifuge, and pH of the supernatants was measured. This process was repeated twice more until the pH of the supernatant was slightly above 8.0, approximately that of the filtered SGW. Following the

third washing with SGW, partial supernatant removal was performed by pipette. Due to differences in the handling of the reaction tubes, some contained more fines in suspension than others. In order to minimize variation in the amount of fines removed with the supernatant, the reaction tubes were oven dried rather than attempting further manual removal of the supernatant. This established uniform solution volume between the reaction tubes prior to the addition of reaction solutions.

The adsorption reactions were carried out in duplicate using five different concentrations of uranium-spiked SGW,  $10^{-7}$  M to  $10^{-5}$  M uranium, as shown in Table 3. An outline of the reaction details can be found in Table 4. The reaction tubes were capped, hand-shaken, and placed on a gentle orbital shaker until the next sample period. Measurements for each sample included pH (Fisher Scientific Accumet Excel XL15 pH meter and Accumet calomel reference electrode, Waltham, MA) and alkalinity (Denver Instrument, Model 295 volumetric titrator, Arvada, CO). Selected cations (Ca, Mg, K, Si, Na) and silicon (Si) concentrations were analyzed using a Perkin Elmer Optima 3300 DV inductively coupled plasma-optical emission spectrometer (ICP-OES) and uranium concentrations using a Perkin Elmer Elan DRC II inductively coupled plasma-mass spectrometer (ICP-MS) (Perkin Elmer, Waltham, MA).

### **2.3. Uranium Leaching Batch Reaction**

In order to understand variation in uranium desorption  $K_{ds}$  and elucidate the mechanisms controlling uranium release from these sediments, static batch leaching reactions were carried out using four leaching solutions; 18.2 megaohms-cm de-ionized water, a (bi)carbonate solution, SGW, and SGW high in sodium and silica. Sediment samples used for these tests were sieved to

remove particles larger than 2mm and oven-dried to unify residual moisture contents. The reaction bottles were capped, hand-shaken, and placed on a gentle mechanical shaker until the next scheduled sample time. For each leaching sample, pH, alkalinity, and selected cations and silica concentrations were measured using the techniques described earlier. Additional details are provided in the subsections below.

### **2.3.1. (Bi)carbonate Leaching**

(Bi)carbonate leaching was performed based on the formation of strong uranium carbonate complexes and associated high mobility of such complexes in soil (Gadelle, et al., 2001; Kohler, et al., 2004; Mason, et al., 1997; Wan, et al., 2009; Wang, et al., 2004). The carbonate leaching solution was prepared using  $1.44 \times 10^{-2}$  M sodium bicarbonate and  $2.8 \times 10^{-3}$  M sodium carbonate, as proposed by Kohler et al., 2004 (Table 2).

### **2.3.2. Synthetic Ground Water With Elevated Na & Si Leaching**

The SGW solution with high sodium and silica concentrations (SGW+Na<sub>2</sub>SiO<sub>3</sub>) was prepared by adding sodium metasilicate to SGW in an amount targeted to exceed the maximum silica concentration leached by previous methods (Table 2). Modeling with *The Geochemists Workbench* (RockWare, Golden, CO) software and small scale saturation tests indicated that saturation of SGW with Na<sub>2</sub>SiO<sub>3</sub> would require nearly 300 g/L Na<sub>2</sub>SiO<sub>3</sub>. The maximum Si concentration leached from the sediments with the other solutions (de-ionized water) was considerably less than this at  $7.96 \times 10^{-3}$  g/L. Clearly, saturation with Na<sub>2</sub>SiO<sub>3</sub> was not required to inhibit Si dissolution. The desired excess silica in solution was targeted at double the

maximum Si dissolved by de-ionized water or  $1.6 \times 10^{-2}$  g/L Si. In order to facilitate potential comparison to the work of others (Ilton, et al., 2008), this concentration was increased to  $2.1 \times 10^{-2}$  g/L Si.

#### **2.4. X-Ray Diffraction**

X-ray diffraction (XRD) was used to elucidate sediment mineralogy. Previously dried samples were sieved to remove particles larger than 53 $\mu$ m. Sieved aliquots were then thoroughly powdered using mortar and pestle, and then packed into separate plastic specimen sample holders. Each sample holder was then scanned using a Scintag PAD V x-ray diffractometer (Cupertino, CA) through 2-theta angular positions of 2 to 65 degrees and operating at 45 kV and 40 mA. Measured X-ray patterns were analyzed using JADE (Materials Data, Inc., Livermore, CA) software (Figure 3).

### **3.0 Results and Discussion**

#### **3.1. Sediment Characterization.**

These sediments exhibit typical sand-dominated, flood sequence characteristics of the H2 unit of the Hanford formation (Hodges and Chou, 2000a; Reidel and Chamness, 2007; Smith, et al., 2001). Particle size analysis revealed that size fractions smaller than 2 mm comprised more than 95% of each bulk sediment sample (Figure 4). Very coarse to very fine sand comprises approximately 90% of these sediment samples, which makes them consistent with the sand-dominated Hanford formation. The remainder is dominated by silt/clay, while particles larger than 2mm account for ~ 0.5% of the bulk sediment.

Most of the core samples collected from direct-push hole C5602 are generally similar with regard to mineralogy and soil texture (Brown, et al., 2007). Similarities in mineralogy between H0B-51.8 and B0A-92.3 can be seen in the XRD profiles (Figure 3). This data indicates the presence of typical Hanford mineralogy in both sediments, including major minerals such as quartz, muscovite, amphibole, albite, and chlorite with minor amounts of pyroxene, hornblende and biotite. Based on the XRD profiles, sample H0B-51.8 differs slightly from B0A-92.3 by the presence of what may be calcite and dolomite. Due to the low content of uranium bearing minerals in the sediment, little can be gleaned from the XRD analysis other than to confirm the similarity between shallow and deep sediment mineralogy.

Based on previous water and acid leachings, uranium concentrations in direct-push hole C5602 sediments were found to decrease with depth (Brown, et al., 2007). Microwave digestion performed on four size fractions shows that the most uranium, as is typical for Hanford sediments, is concentrated in the finest size fractions (Cantrell, et al., 2003; Krupka, et al., 2004; Last, et al., 2006; Zachara, et al., 2007a) (Figure 5) and that the lower limit of the contaminant plume front is between 83.3' bgs and 91.8' bgs. Evidence of this assertion can be found in comparison of sediment total uranium concentrations found from microwave digestion (Table 1). Total uranium concentrations of 1.4 – 5.1  $\mu\text{g/g}$  are considered to be typical of natural background uranium concentrations in Hanford sediments (Brown, et al., 2007; Zachara, et al., 2007a).

### 3.2. Uranium Adsorption Batch Reaction

Within the range of  $10^{-7}$  M to  $10^{-5}$  M uranium, U-spiked SGW reactions with B0A-91.8 reached adsorption kinetic equilibrium within a week, or less (Figure 6). The  $10^{-5}$  and  $10^{-6}$  M uranium solutions reached maximum adsorption, within the range of the standard deviation, by day two. The less concentrated uranium solutions had much lower sample standard deviations and reached maximum sediment adsorption in less than 24 hours. The initial pH of the uranium spiked solutions ranged from 6.5 to 7.5, depending on the concentration of uranium nitrate solution that was added in order to achieve the desired uranium concentration. Initial solution pH rose with decreasing uranium nitrate concentration. Within one hour of reaction start, solution pH in all reactor vessels had equalized to a range between 7.8 – 7.9. By reaction end, at 14 days, solution pH remained only slightly higher at 8.0 – 8.1 (Figure 7). Alkalinity also remained relatively stable throughout the course of the adsorption reaction. Alkalinity generally ranged from 80 to 115 mEq/L (Figure 8). Variability in alkalinity measurements is greater than that of pH. But when viewed within the context of the standard deviations, the alkalinity measurements varied little from the average of 95 mEq/L. Reasonable pH and alkalinity stability throughout the reaction period points to comparatively similar and stable adsorption conditions. Such stable conditions validate the comparison, between the different U-spiked solutions, of adsorbed uranium on the background sediment B0A-91.8.

This sediment exhibited a linear adsorption trend for solutions ranging from  $10^{-7}$  M to  $10^{-5}$  M uranium, (Figure 9) with a derived  $K_d$  value of 2.1 L/Kg. However, since the sediment's maximum adsorption capacity was not achieved, this  $K_d$  value would be better interpreted as a lower limit rather than a realistic  $K_d$ . As such, this value is around 2 orders of magnitude lower than previous desorption  $K_d$  estimates for the same sediment (Brown, et al., 2007). However,



this value is not outside the wide range of  $K_{ds}$  (0-100 or more) that might be expected for a Hanford sediment in groundwater (Cantrell, et al., 2003; Last, et al., 2006; Zachara, et al., 2007a). Experimental U-isotherm data was initially used to fit to Langmuir and Freundlich isotherm models using a least squares approach. The calculation was done using a “solver” function in a spreadsheet table to provide the modeled data points for a graph comparing modeled and experimental points. Because the graph updates automatically, this method provided the opportunity to manipulate the variables and get instant feedback on how they affect the outcome of the model. The Langmuir model is represented by the equation:

$$C' = aC/(1+bC) \quad (3.1)$$

Where  $C'$  = weight of the sorbate divided by the dry weight of the sorbent

$a$  = a constant

$C$  = solute concentration in solution

$b$  = adsorption rate constant

The Freundlich model is represented by the equation:

$$C' = K_f C^n \quad (3.2)$$

Where  $K_f$  = the Freundlich distribution coefficient

$n$  = a constant

Use of the least squares approach seemed reasonable given the limitations of the experimental data. Also, the linear experimental data are only relevant to the initial linear portion of typical isotherms for each model. Graphic results revealed that either model could be a reasonably good fit, although the Freundlich yielded a higher sum of least squares ( $8.5 \times 10^{-8}$ ) than the Langmuir ( $7.1 \times 10^{-9}$ ). The Langmuir equation returned constant values of  $a = 2.4 \times 10^{-3}$  and  $b = 0.1$  for the linear segment of the curve. These values result in a maximum loading capacity of  $2.4 \times 10^{-2}$  mg

U/g sediment. The Freundlich equation returned constant values of  $K = 2.4 \times 10^{-3}$  and  $n = 0.80$ .

When  $n$  is equal to a positive number, as in this case, it means that the slope of the equation is positive and adsorption will occur. If a negative value for  $n$  had been found, then the slope of the equation would have been negative and desorption would have been the mechanism involved.

Based on comparison of the sum of least squares, the Langmuir equation provides a better model for the experimental data. This is not surprising considering that the Langmuir equation accommodates the approximation of more complex experimental data by providing a means of representing a maximum sorption value as the sorbate concentration continues to rise. However, the point of maximum sorption was not reached in this case. Because the experimental data are limited to such a small range of uranium concentrations and both Freundlich and Langmuir equations have linear segments at low initial concentrations, it is not surprising that  $K_d$ s might be similar over this range. However, at higher concentrations,  $K_d$ s would be expected to diverge as the Freundlich  $K_d$  continued to rise while the Langmuir  $K_d$  eventually reached a maximum value.

In order to further check the fit of the experimental data to the Freundlich and Langmuir models, the data was compared to the linear form of each equation. The linear form of Freundlich equation (3.2) can be written as:

$$\text{Log } C' = \text{log } K + n \text{ log } C \quad (3.3)$$

If the model is a good fit, graphing experimental values of  $\text{log } C'$  vs  $\text{log } C$  (Figure 10) should result in a linear trend. This was indeed the case, with a regression coefficient ( $R^2$ ) value of 0.9695 indicating a good fit between the experimental data and the trendline. When this same comparison is made using the linear form of the Langmuir equation (3.1):

$$1/C' = (b/a) + (1/aC) \quad (3.4)$$

graphing  $C/C'$  vs  $C$  (Figure 11) did not yield a good fit between the experimental data and the

trendline. Comparing the resultant value of  $R^2 = 0.0561$  to that of the linear Freundlich, it is clear that the Freundlich model is a much better fit to the experimental data. While the least squares approach is instructive in its illustration of the dynamic relationship between the variables and the isotherm, it apparently does not capture the more subtle nuances. Modeling the experimental data through use of the linear form of the Freundlich and Langmuir equations provides more defensible results.

However, it has been suggested that a linear  $K_d$  approach is insufficient for modeling the complex chemical environment resulting from the release of highly contaminated, acidic or alkaline wastes, as is typical of tank wastes, to Hanford sediments (Last, et al., 2006; Um, et al., 2007; Um, et al., 2009). The linear  $K_d$  approach to adsorption modeling is a simple model with only two variable parameters. This simplicity makes it easy to predict sorption rates within the confines of the limited conditions it represents. But, it assumes that sediment adsorption capacity is unlimited. This can lead to an overestimation of the sediment's sorption capacity to the sorbate, if used to extrapolate outside the existing data. In that it is not strictly linear, the Freundlich sorption isotherm is a better model for the non-linear portion of a given data set. But, it does not account for the finite nature of sorption sites on real sediments. The Langmuir isotherm addresses this issue and should be the preferred model, provided sufficient data regarding the maximum sorption capacity of the sediment is included. With respect to sediment B0A-91.8, the maximum sorption capacity was not reached so the benefit of the Langmuir isotherm could not be realized. Due to the limitations of the experimental data set, the Freundlich isotherm appears to be a better model when, in fact, it should not be as accurate for a more inclusive data set with non-linear  $K_d$ s at higher concentrations on the sediment. Therefore, a more inclusive experimental and modeling approach with regard to transport mechanisms would

provide a more useful set of  $K_{ds}$  that more closely approximated contaminant phase conditions found in actual field conditions.

Given that this sediment probably did not realize the maximum uranium adsorption capacity within this range of uranium concentrations, it would be useful to further develop uranium adsorption characterization by conducting a similar experiment with the same sediment while using a higher range of uranium concentrations. This could provide a reasonably clear indication of the maximum adsorption capacity of this sediment and would provide a basis from which adsorption could be modeled for comparison and potential application to other sediments.

### **3.3. Uranium Leaching Batch Reaction**

The rate of uranium leached from all sediments with the different solutions was greater during the initial period of about 14 days and increased less steeply thereafter, suggesting two modes of uranium release, such as initial rapid uranium desorption followed by dissolution of uranium bearing minerals. More specifically, batch reactions revealed one or more components of the most shallow and contaminated sediment, H0A-52.3, that released relatively large amounts of uranium in the (bi)carbonate solution and SGW. While the amount of uranium leached with the (bi)carbonate solution at 90 days was roughly three times that of the SGW solution, the trend, in each case, was one of increasing uranium leaching that did not appear to approach equilibrium. Throughout these reactions, pH and alkalinity remained relatively flat after initial stabilization periods, which allowed reasonable comparisons to be made between reactions. Ending pH values for each of the reactions was quite stable with the exception of the (bi)carbonate reaction, which was a little higher than the rest at about 9.3 (Table 2).

### 3.3.1. De-ionized Water Leaching

In this reaction the release of Si and U were very similar to that of SGW for all sediments except H0A-52.3 (Figures 12, 13, 14). In this case, U release was suppressed very close to that of intermediate sediment H2A-83.3 (Figure 12). This suggests similarity in the U reservoir tapped by DI water in these sediments. In both cases U equilibrium was approached within a week indicating that desorption is a likely primary mechanism, although slight continual release through 90 days was apparent. Calcium was released from all of the sediments at comparable rates through 14 days, after which Ca concentrations diverged slightly with the intermediate depth sediments being similar to each other and the shallowest and deepest sediments being similar to each other (Figure 13). Initial release of similarly desorbed Ca through 14 days may have been followed by divergent Ca dissolution products. It seems apparent that the nature of calcium in the intermediate depth sediments has been somehow altered from that of the deep, background sediment but this same alteration does not seem to apply to the shallowest sediment which would otherwise be considered to be the most contaminated. This raises the question of whether or not the intermediate and shallow sediments have been subjected to the same contaminant waste streams. If not, the differences may be due to chemical alteration of the waste stream as it moves downward through the vadose zone or possibly the intermediate sediments were contacted with a different waste stream through lateral flow at depth. Regardless, there was a similar pattern observed from the preliminary uranium  $K_d$  estimates in which release was similar between shallow and deep sediments and decidedly different for intermediate sediments. Based on these observations, it seems possible that there may be a link between the nature of

calcium in these sediments and their respective uranium release rates, but further evidence is still needed.

### **3.3.2. (Bi)carbonate Leaching**

The primary purpose of this batch reaction was to distinguish the labile U fraction that is easily and rapidly desorbed from sediment from the more recalcitrant uranium that is more slowly released over time due to dissolution. This concept and the method employed here are well detailed by Kohler et al 2004. If labile U can be quantified in this way, then dissolved U can be more easily identified for this same sediment in other solutions. For H0A-52.3, the ratio of labile uranium leached with the (bi)carbonate solution, at 90 days, to total uranium as found through microwave digestion was  $\geq 1.1:1$ . It seems that the distinction between easily desorbed uranium and early-stage dissolution has been somewhat blurred. This apparent overestimation of labile uranium by (bi)carbonate leaching could be problematic if not modified by other experimental data. This could be especially true for sediments that include both adsorbed and precipitated forms of uranium, and uranium silicates which are easily dissolved at high pH. Both conditions were suspected to be the case with these sediments. Under these conditions, isotopic exchange might provide a more reliable estimate of labile uranium. In spite of this potential shortcoming when using this (bi)carbonate leaching process to estimate labile uranium, there did appear to be two distinctly different uranium release rates for sediment H0A-52.3 in this solution. As can be seen in Figure 15, there was a period of rapid uranium release lasting at least 7 days followed by a period of more slowly but steadily increasing uranium release through the end of the 90 day reaction period. There is an apparent inflection point in the curve of uranium

release between 7 and 10 days that may mark the transition between uranium release through desorption and dissolution. Correspondingly, in Figure 16, there may be a similar inflection point between 7 and 10 days with regard to silica released by the (bi)carbonate solution. This implies a link between uranium and silica release rates and that the slower release rate after 10 days reaction time may result from dissolution of uranium silicate. However, U release at the end of the reaction period is roughly twice that of Si and Ca (Figure 17) suggesting that the source of uranium release by the (bi)carbonate solution is not closely linked to either Ca or Si. Throughout the reaction period with the (bi)carbonate solution, sediment H1A-68.3 released noticeably more silica than did the other sediments. This implies a link between U and Si in this sediment that seems to be lacking in the other sediments.

### **3.3.3. SGW Leaching**

While the other sediments appeared to have reached equilibrium with uranium within a week, H0A-52.3 experienced rapid uranium release over the first 14 days, followed by more moderate but continual release through the end of the 90 day reaction period (Figure 18). The continued increase of Ca and Si leaching concentrations from H0A-52.3 in SGW at 90 days also suggests uranium association with these elements and would be consistent with uranophane as the dominant form of uranium (Figure 19 and 20).

After 90 days of reaction time with the SGW solution, sediment H0A-52.3 had released one to two orders of magnitude more uranium than the other sediments. With this sediment there was good correlation between Si and U release (Figure 21). Concentrations of the two ions were very similar through 14 days reaction time. While they began to gradually diverge thereafter,

both continued to rise at nearly parallel rates through 60 days, after which Si may have been approaching equilibrium. This may suggest three release mechanisms; 1) uranium desorption through 14 days, 2) some combination of uranium desorption and dissolution through 60 days, 3) some other uranium dissolution product after 60 days.

Sediment H1A-68.3 reached uranium equilibrium within one week while Si release continued through the 90 day reaction period (Figure 22). Release profiles were generally similar for H2A-83.3 except that U concentrations were lower and approaching equilibrium at 30 days, and Si appeared to be approaching equilibrium at 60 days (Figure 23). Release concentrations of Si and U in B0A-92.3 sediment were similar but lower than intermediate depth sediments H1A-68.3 and H2A-83.3, although silica began to approach equilibrium at 30 days (Figure 24). For sediments H1A, 68.3, H2A-83.3, and B0A-92.3 there was no apparent correlation between uranium and silica release.

#### **3.3.4. SGW+Na<sub>2</sub>SiO<sub>3</sub> Leaching**

Uranium release from H0A-52.3 was suppressed in SGW containing elevated Na and Si ions (Figure 25), approaching equilibrium in 30 days at a concentration nearly an order of magnitude lower than that of SGW (Figure 18). This suggests the dominant presence of a uranium silicate in this sediment and supports the earlier fluorescence spectroscopy findings of Um et al. 2009 that suggested the dominant uranium phase in this sediment was similar to natural uranophane and boltwoodite. While uranium leached from H0A-52.3 in SGW+Na<sub>2</sub>SiO<sub>3</sub> was approaching equilibrium at 30 days, the concentration of uranium released from H1A-68.3 continued to increase up to 90 days (Figure 25). This suggests the dominant form of uranium in



H1A-68.3 is different than that of H0A-52.3 and may support the earlier conclusion that these intermediate sediments may be dominated by adsorbed U(VI) rather than U-silicate mineral precipitates (Um, et al., 2009). Furthermore, this may also be a significant source of long term uranium release. Based on HA-68.3 uranium release as illustrated in Figure 25, there may be two distinct release mechanisms at work. Within the first 3-4 days, the released uranium concentration increases rapidly and then reaches a temporary plateau until sometime after 30 days of reaction. After this time, released uranium begins to increase again, although at a lower rate than for that of the initial 3-4 days. This profile suggests an initial 3-4 day period of rapid uranium release due to desorption followed by a 26 day period during which uranium release by dissolution has not yet had time to occur. After 30 days a uranium dissolution threshold may have been met, resulting in uranium release at an increasing rate for at least the next 60 days – which was the end of the experimental sampling period. The initial 3-4 day uranium fast-release from this sediment corresponds to an initial rapid loss of Ca from solution (Figure 26). The Ca concentration in solution remains relatively constant thereafter. In contrast, Si concentrations are relatively stable throughout the 90 day experimental period (Figure 27). This indicates that dissolution of whatever uranium phase may be involved is unlikely to include a uranium silicate as was indicated for the shallower sediment H0A-52.3.

#### **4.0 Conclusions**

All sediments from this direct-push hole, except the deep background samples, contain elevated levels of uranium (Table 1). It is clear that uranium bearing Hanford wastes have interacted with these sediments. It is likely that multiple forms of uranium have been immobilized, to various degrees, within these sediments. The goal is to determine which

uranium release mechanisms are involved with the hope that they might also shed light on the nature of uranium uptake by the sediments. Motivated by the observation that shallow and deep sediments from this direct-push hole had similar  $K_d$  estimates, yet distinctly higher  $K_{ds}$  than intermediate sediments, and the desire to understand this apparent paradox, the primary objective has been to confirm the presence of uranium silicate mineral precipitates in sediment H0A-52.3 and to illustrate its dominance as a driver of long-term uranium release to the vadose zone and ground waters.

The rate of uranium leached from all sediments with the different solutions was greater during the initial period of 7-14 days and increased less steeply thereafter, suggesting two modes of uranium release, such as initial rapid uranium desorption potentially followed by dissolution of uranium bearing minerals. This two stage release process was most clearly illustrated by batch reactions using (bi)carbonate solution, SGW solution, and SGW+Na<sub>2</sub>SiO<sub>3</sub> solution. Sediment H1A-68.3 illustrated this point in the SGW+Na<sub>2</sub>SiO<sub>3</sub> solution where the uranium release curve displays a clear and obvious plateau between 10 and 30 days reaction time before increasing through the remainder of the reaction period of 90 days. This implies release mechanisms of initial uranium desorption through 7-10 days followed by a period of very little uranium release due to the time required for dissolution processes to occur. Once dissolution begins to occur near 30 days, the process has the potential to be a source of long term vadose zone uranium migration. Because dissolved uranium can account for 30-50% or more of all mobile uranium in the most contaminated sediments, a thorough understanding of the mechanisms involved is a key component of mitigation. However, it is unlikely that this source of long-term uranium release in sediment H1A-68.3 is a uranium silicate because dissolution of silicates was strongly inhibited by the high silica content of the leaching solution. In the

(bi)carbonate and SGW solutions, sediment H0A-52.3 dramatically illustrated the concept of multiple uranium release mechanisms. In each case, uranium release was highly elevated above that of the other sediments and two distinct release rates can be seen in the slope of the curves before and after 14 days of reaction time. Initial fast-release of uranium may be dominated by desorption through 14 days followed by predominantly uranium bearing mineral precipitate dissolution through the end of the reaction period of 90 days. Again, this late-term uranium dissolution product has the potential to be a secondary source of long-term uranium migration through the vadose zone to groundwater. The (bi)carbonate solution did not provide a clear and quantifiable differentiation between labile and precipitated uranium, especially for the sediments containing U-silicate precipitates. The inflection point in the release curve between 14 and 20 days of reaction time is a strong indicator that there are two mechanisms at work in sediment H0A-52.3. A similar conclusion can be drawn from the profile of the uranium release curve for this sediment in SGW. Further comparison of uranium release from this sediment in SGW to that in SGW+Na<sub>2</sub>SiO<sub>3</sub> illustrates the suppression of uranium release in the latter solution high in Si. If the solution has a high initial Si concentration, then its capacity to dissolve more Si is diminished. If the late-term uranium dissolution product observed in SGW is suppressed in a high Si solution, then this uranium source in the sediment can be correlated to a uranium mineral bearing precipitate with significant silica content. This supports the earlier findings that, within shallow contaminated sediments, uranium bearing mineral precipitates such as uranophane and boltwoodite may be significant in their long term contribution to vadose zone uranium migration. However, in light of the lack of correlation between U and Si release in the bicarbonate solution it seems likely that there may be two primary forms of long term U release in sediment H0A-52.3. One is closely linked to the release of Si as illustrated by leaching with SGW and

SGW+Na<sub>2</sub>SiO<sub>3</sub>. The other source of long term U release, revealed with the (bi)carbonate solution is unrelated to Si release.

The nature of uranium contained within the sediments of direct-push hole C5602 clearly varies by depth. The shallow sediment H0A-52.3 likely contains, adsorbed uranium, some type of uranium silicate mineral precipitate, and a form of uranium that is not closely linked to Si. The intermediate depth sediment H2A-68.3 also suggests an adsorbed uranium component in addition to a more slowly released form of uranium for which release is not hindered by high Si in solution. It remains to be determined whether these differences may be due to chemical alteration of the waste stream as it moves downward through the vadose zone or potential intermediate depth sediment contact with a different waste stream through lateral flow at depth.

## **Acknowledgment**

This research was supported by Pacific Northwest National Laboratory (PNNL). PNNL is operated for the U.S. Department of Energy by Battelle Memorial Institute under Contract DE AC05 76RL01830. Special thanks go to all of the staff in PNNL's Applied Geology and Geochemistry group. Assistance was provided by Washington State University, School of Earth and Environmental Sciences.

## Appendix

Table 1 Sediment samples from direct push hole C5602.

Sample ID	Sample Depth (ft bgs)	Total U		Leached U at 90 days				U:Total U Labile
		from Microwave Digestion ( $\mu\text{g/g}$ )	from acid leaching <sup>a</sup> ( $\mu\text{g/g}$ )	DI ( $\mu\text{g/g}$ )	SGW ( $\mu\text{g/g}$ )	SGW + $\text{Na}_2\text{SiO}_3$ ( $\mu\text{g/g}$ )	(Bi) carbonate ( $\mu\text{g/g}$ )	
H0B-51.8	51.8	6.65E+02	7.31E+02	8.43E+00	1.70E+02	2.20E+01	4.89E+02	$\geq 1.1:1$
H0A-52.3	52.3	4.27E+02	4.14E+02	8.43E+00	1.70E+02	2.20E+01	4.89E+02	$\geq 1.1:1$
H1B-67.8	67.8	1.42E+01	1.52E+01	1.89E+01	2.58E+01	3.90E+01	2.49E+01	$\geq 0.8:1$
H1A-68.3	68.3	3.16E+01	3.11E+01	1.89E+01	2.58E+01	3.90E+01	2.49E+01	$\geq 0.8:1$
H2B-82.8	82.3	2.98E+01	2.09E+01	5.81E+00	8.99E+00	7.75E+00	8.41E+00	$\geq 0.6:1$
H2A-83.3	83.3	1.41E+01	1.16E+01	5.81E+00	8.99E+00	7.75E+00	8.41E+00	$\geq 0.6:1$
B0B-91.8	91.8	1.40E+00	4.97E-01	1.04E-01	3.99E-02	4.31E-03	2.93E-02	$\geq 0.02:1$
B0A-92.3	92.3	1.54E+00	3.86E-01	1.04E-01	3.99E-02	4.31E-03	2.93E-02	$\geq 0.02:1$

<sup>a</sup> Brown et al 2007

Table 2. Chemical recipe for experimental solutions.

Chemical	De-ionized Water	(Bi)carbonate (M)	SGW (M)	SGW + Na & Si (M)
Na	na	0.02	1.53E-03	4.92E-02
Ca	na	0	2.86E-04	2.86E-04
Mg	na	0	5.29E-04	5.29E-04
K	na	0	4.30E-04	4.30E-04
Si	na	0	0	7.47E-04
CO <sub>3</sub>	na	0.0028	1.05E-03	1.04E-03
HCO <sub>3</sub>	na	0.0144	1.03E-03	1.03E-03
SO <sub>4</sub>	na	0	9.81E-04	9.81E-04
NO <sub>3</sub>	na	0	5.71E-04	5.71E-04
initial solution				
pH	6.6	9.3	8.16 <sup>b</sup>	9.67 <sup>c</sup>
reaction end	8.3-8.6			
pH		9.2-9.4	8.0-8.5	8.4-8.6

<sup>b</sup> post saturation with CaCO<sub>3</sub> and filtration of excess precipitate

<sup>c</sup> post saturation and filtration of excess CaCO<sub>3</sub> followed by addition of Na<sub>2</sub>SiO<sub>3</sub>



Table 3. Synthetic ground water (SGW) uranium spike concentration.

Target uranium concentration (M)	Target uranium concentration ( $\mu\text{g/L}$ )	Measured uranium concentration ( $\mu\text{g/L}$ )
1.00E-05	2.38E+03	2.20E+03
5.00E-06	1.19E+03	1.09E+03
1.00E-06	2.38E+02	2.20E+02
5.00E-07	1.19E+02	1.10E+02
1.00E-07	2.38E+01	1.97E+01

Table 4. Reactor Setup.

Process (In Duplicate)	Reaction Vessel (mL)	Sediment (g)	Solution (mL)	Solid to Solution Ratio	Reaction Time(days)	Sample Size (mL)	Sample Filtration ( $\mu\text{m}$ )
Adsorption	50	3	30	1:10	90	3	0.45
DI Extraction	50	0.5	50	1:100	90	5	0.45
SGW Extraction	50	0.5	50	1:100	90	5	0.45
SGW+Na <sub>2</sub> SiO <sub>3</sub> Extraction	50	0.5	50	1:100	90	5	0.45
(Bi)carbonate Extraction	250	2	200	1:100	90	2	0.45

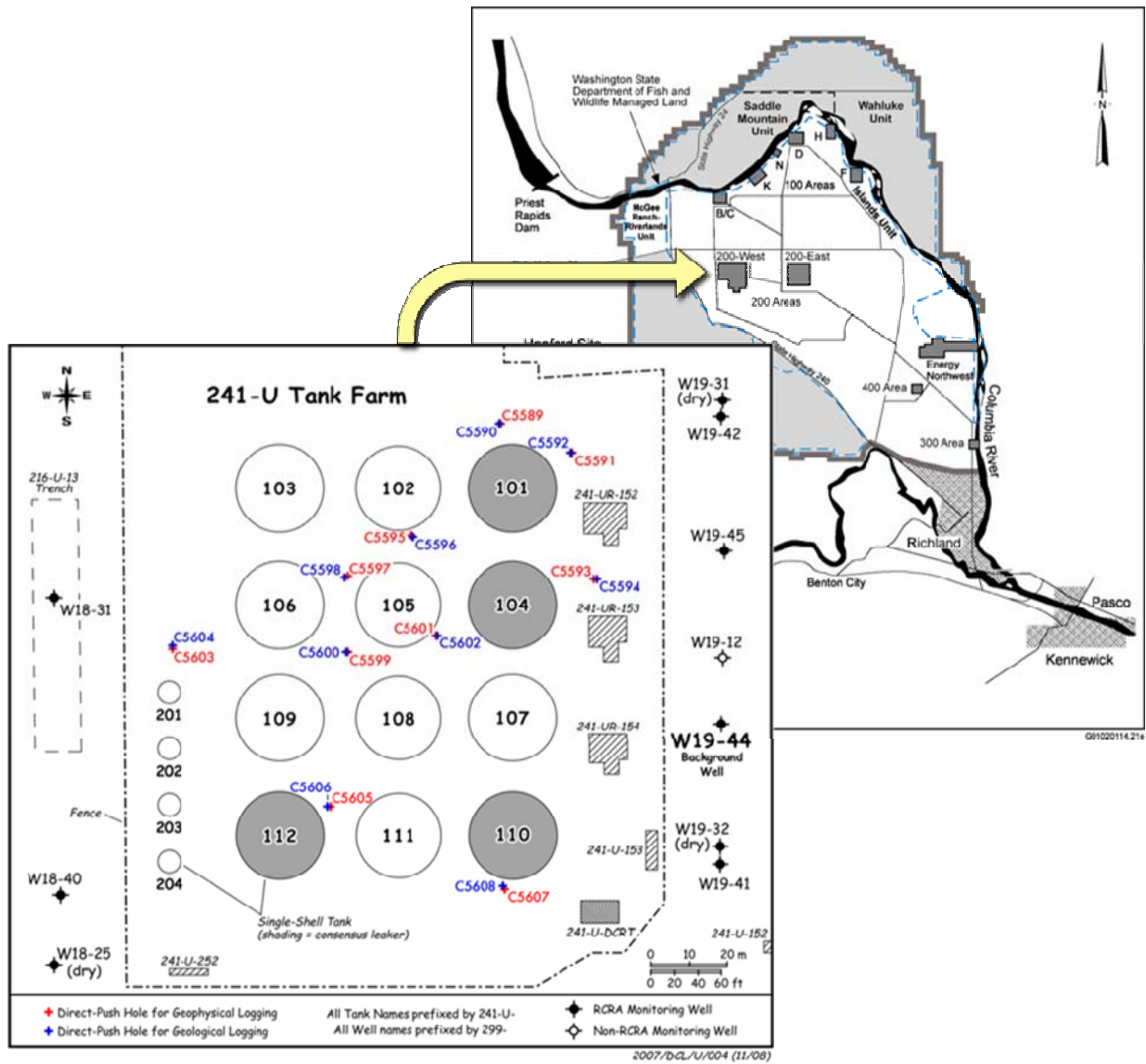


Figure 1. Location map of the U tank farm at the Hanford Site.

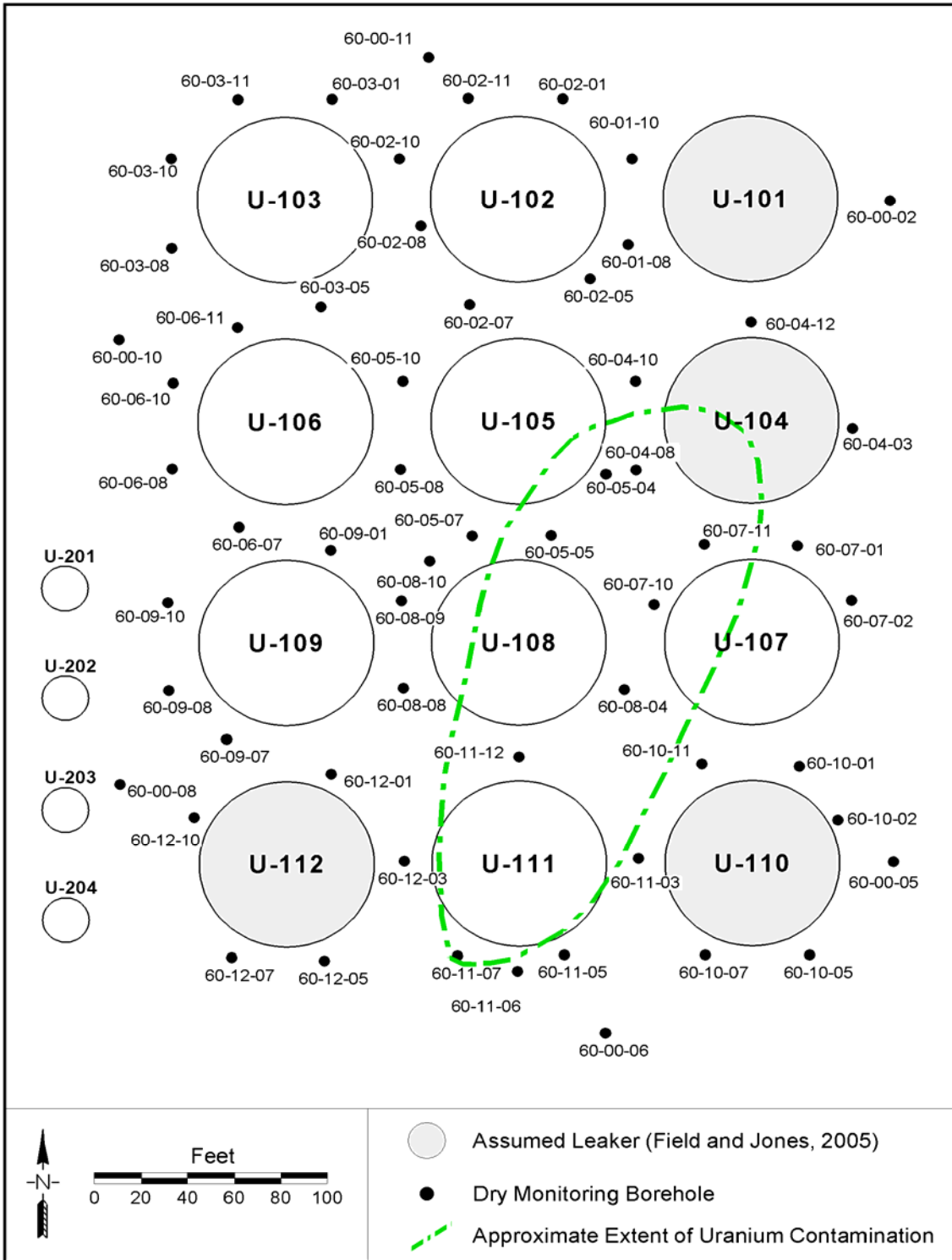


Figure 2. Tank U-104 uranium plume (Crumpler 2004).

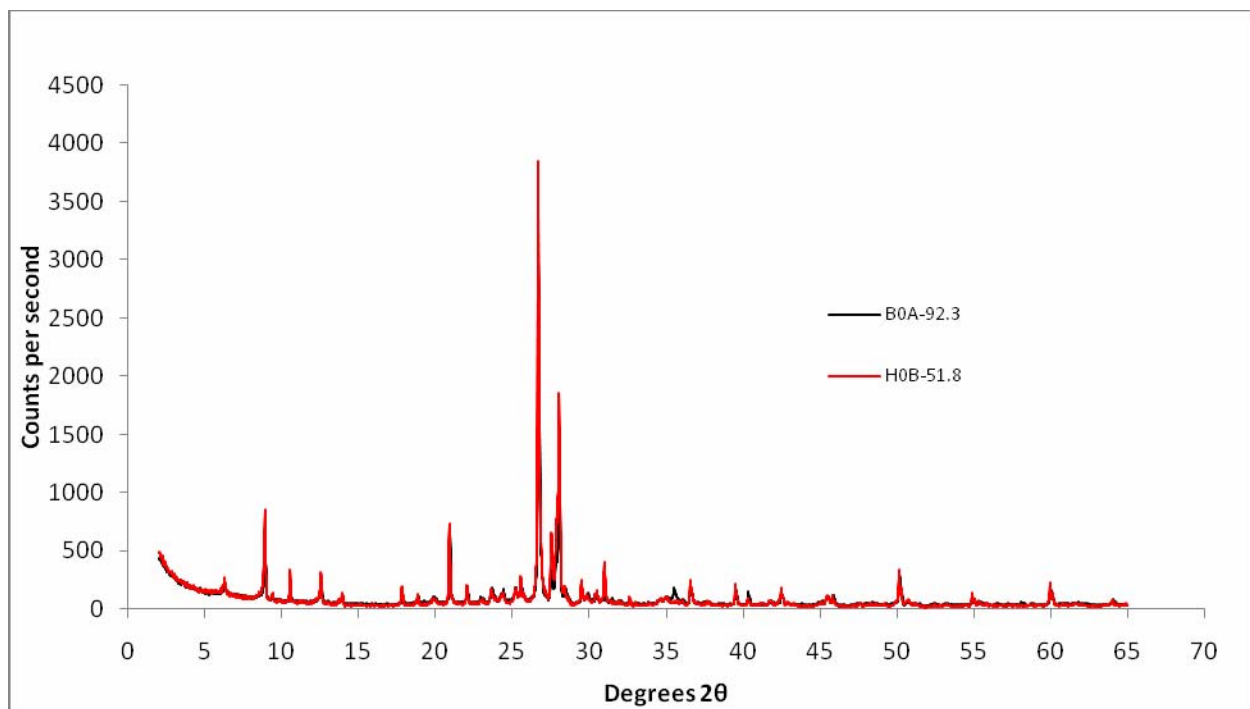


Figure 3. XRD analysis of H0B-51.8 as compared to B0A-92.3

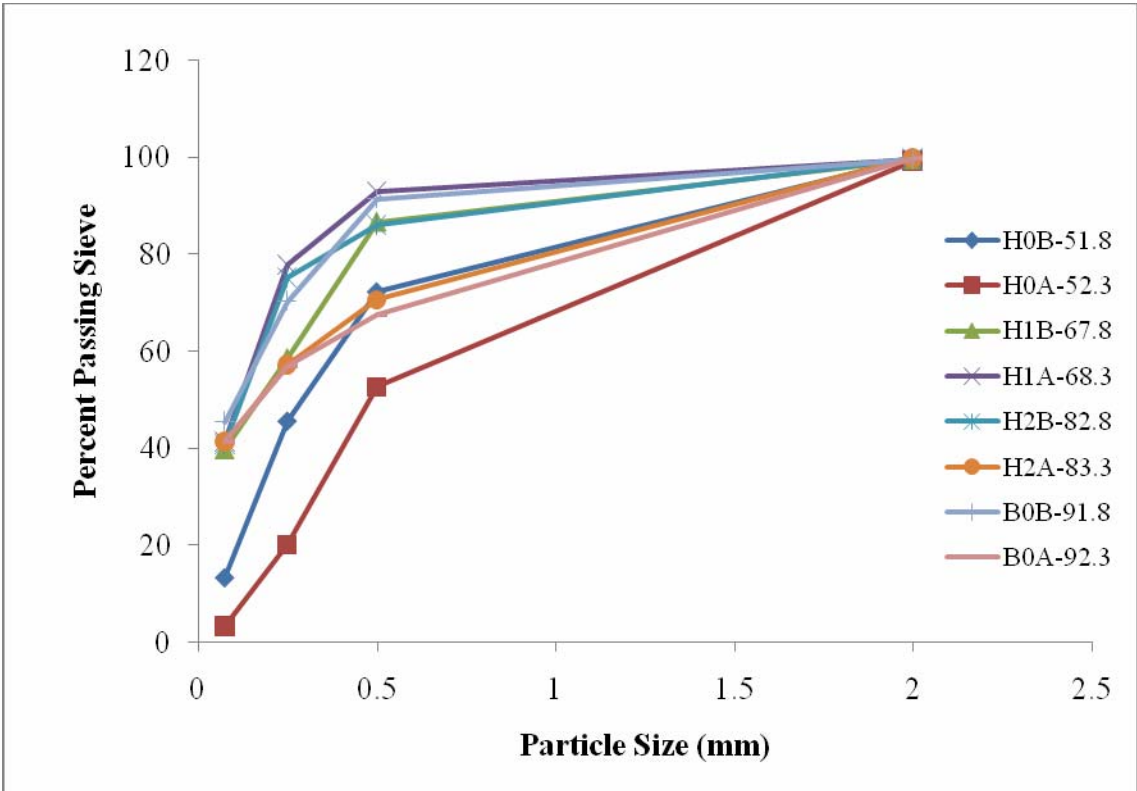


Figure 4. Particle size distribution of C5602 sediments.

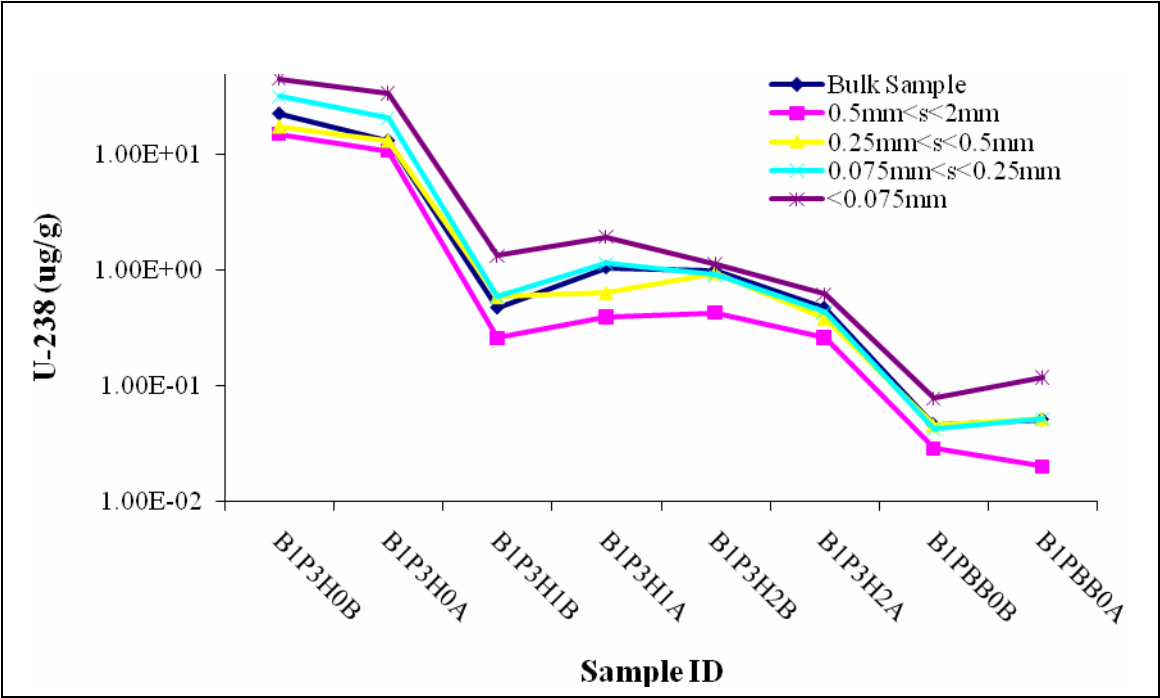


Figure 5. Total uranium content by size fraction as determined by microwave digestion.

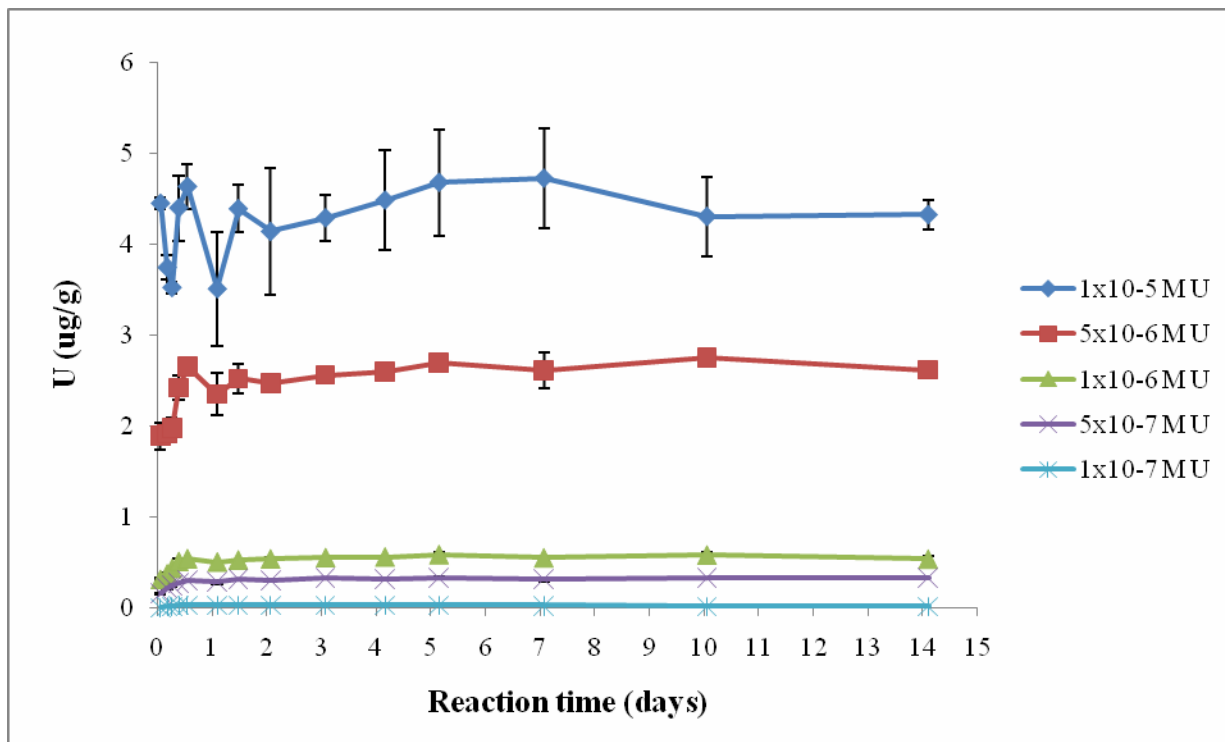


Figure 6. Uranium adsorption on B0A-91.8 in U-spiked SGW.



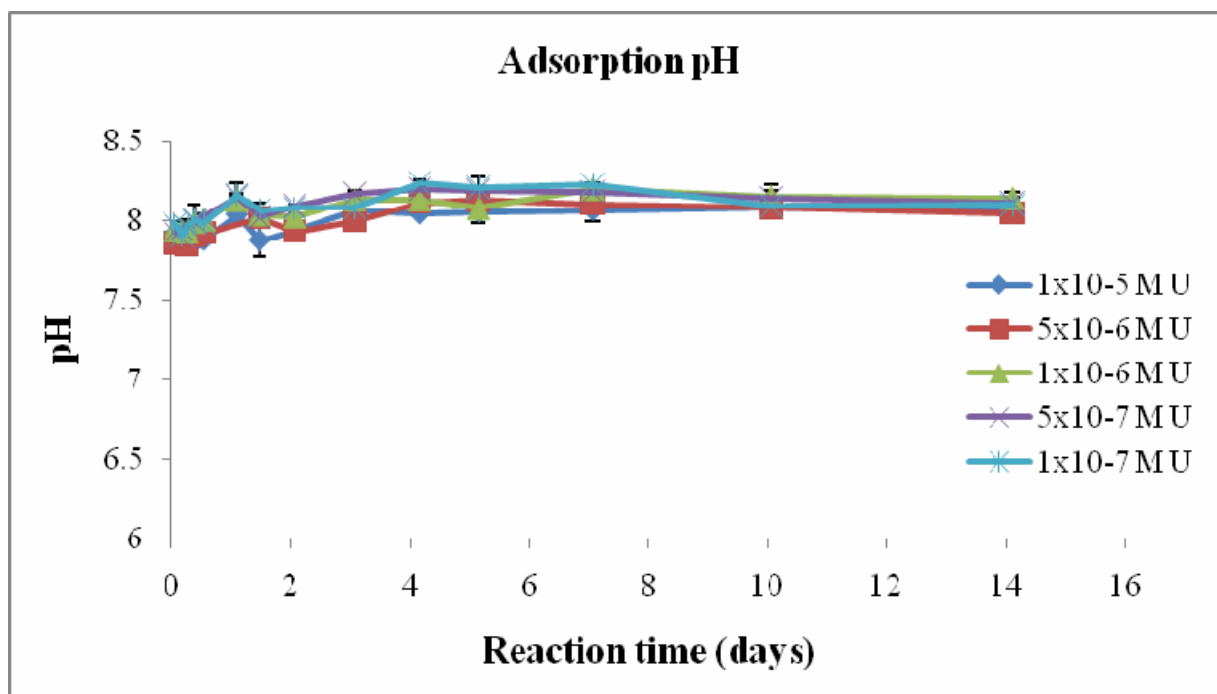


Figure 7. Adsorption reaction pH.

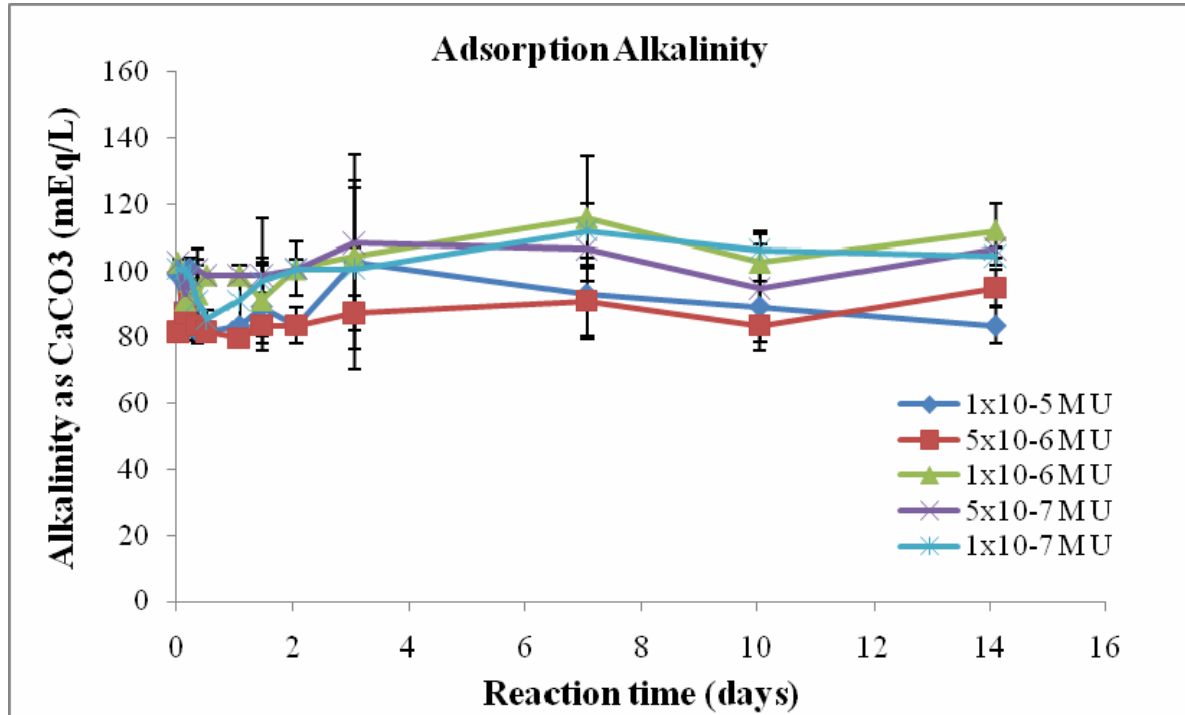


Figure 8. Adsorption reaction alkalinity.

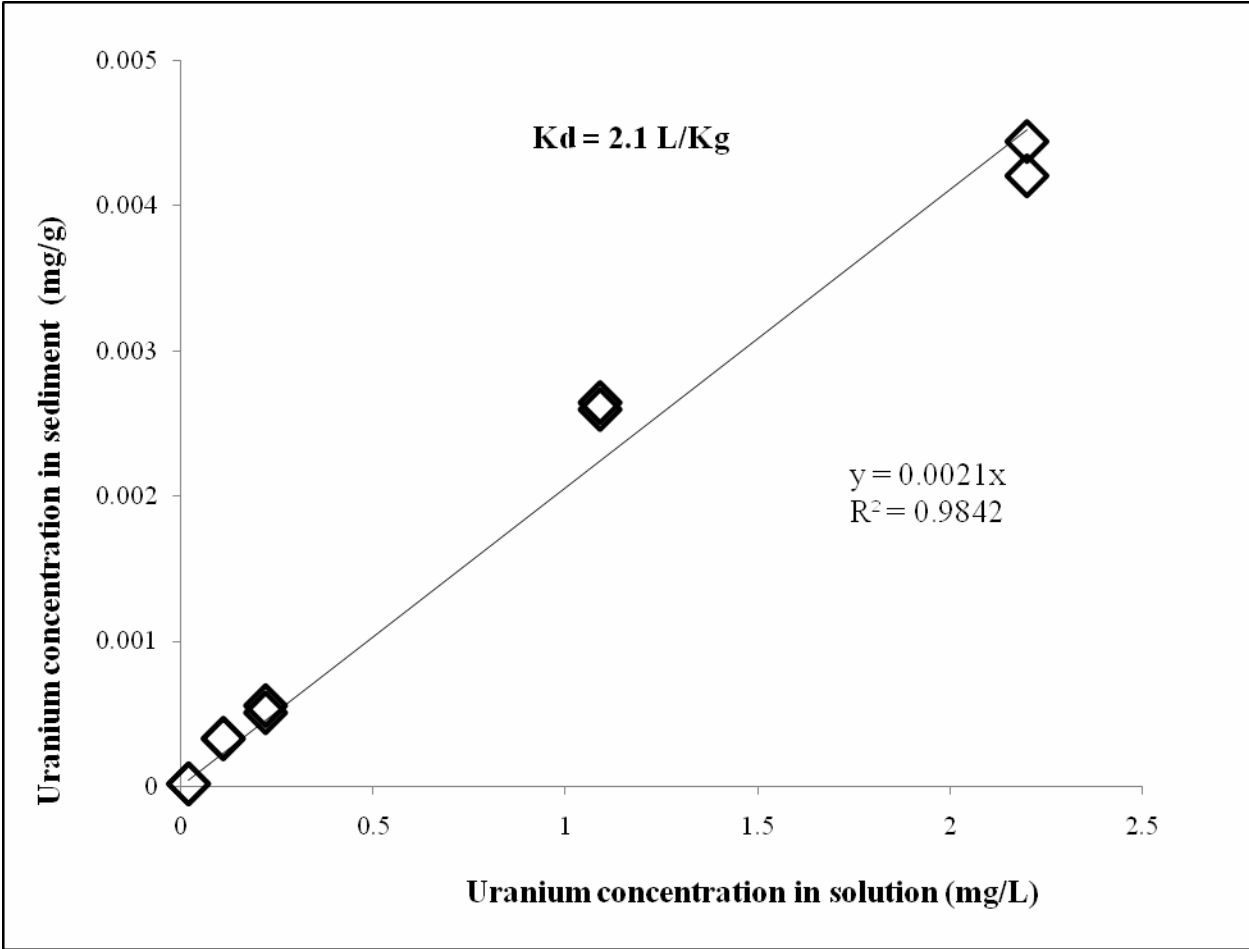


Figure 9. B0A-91.8 adsorption isotherm at fourteen days.

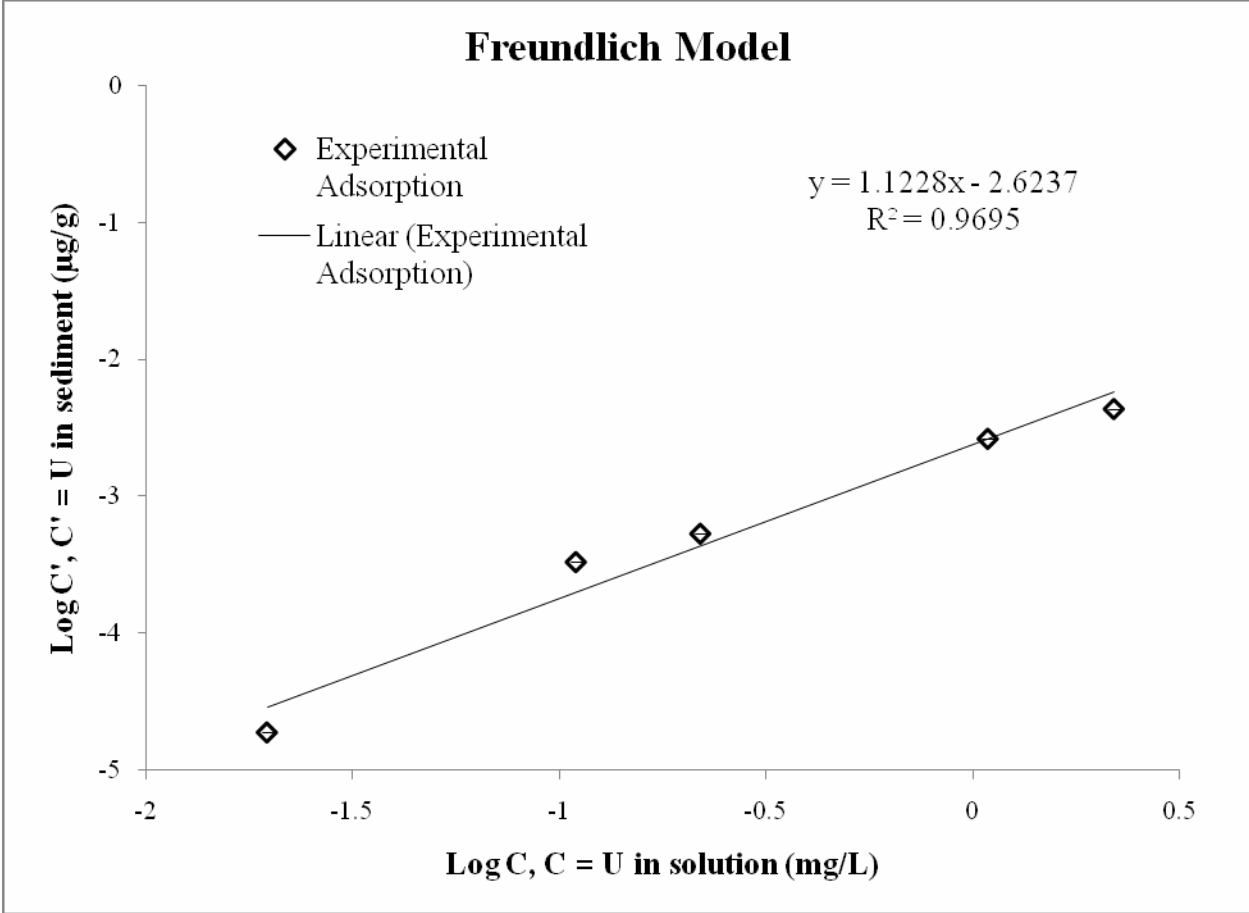


Figure 10. Experimental data fit to linear form of Freundlich equation.

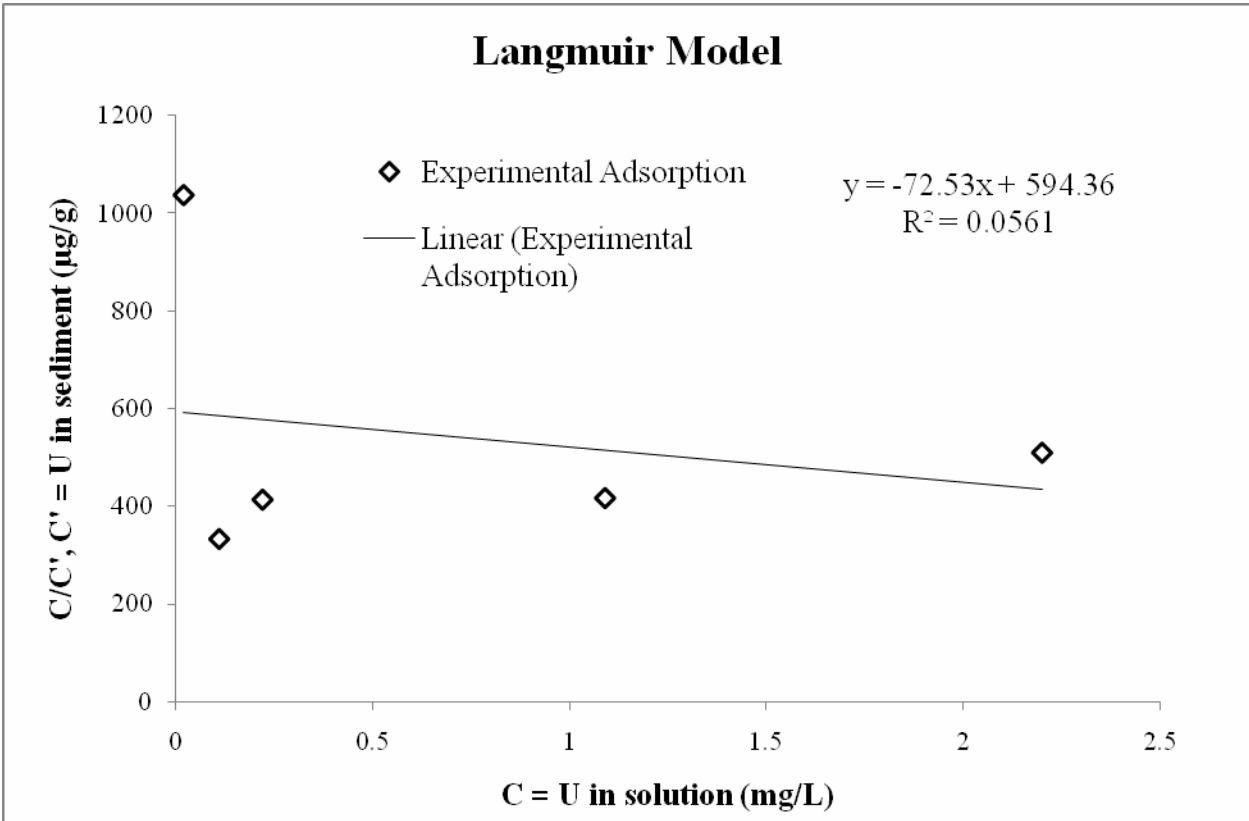


Figure 11. Experimental data fit to linear form of Langmuir equation.

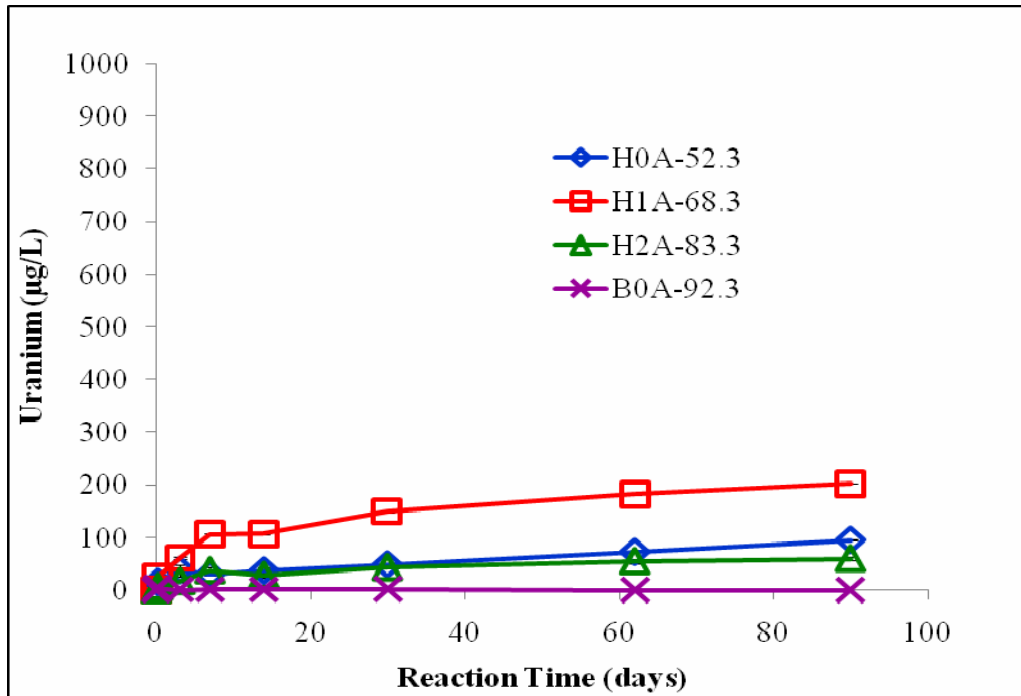


Figure 12. De-ionized water leaching, uranium in solution.

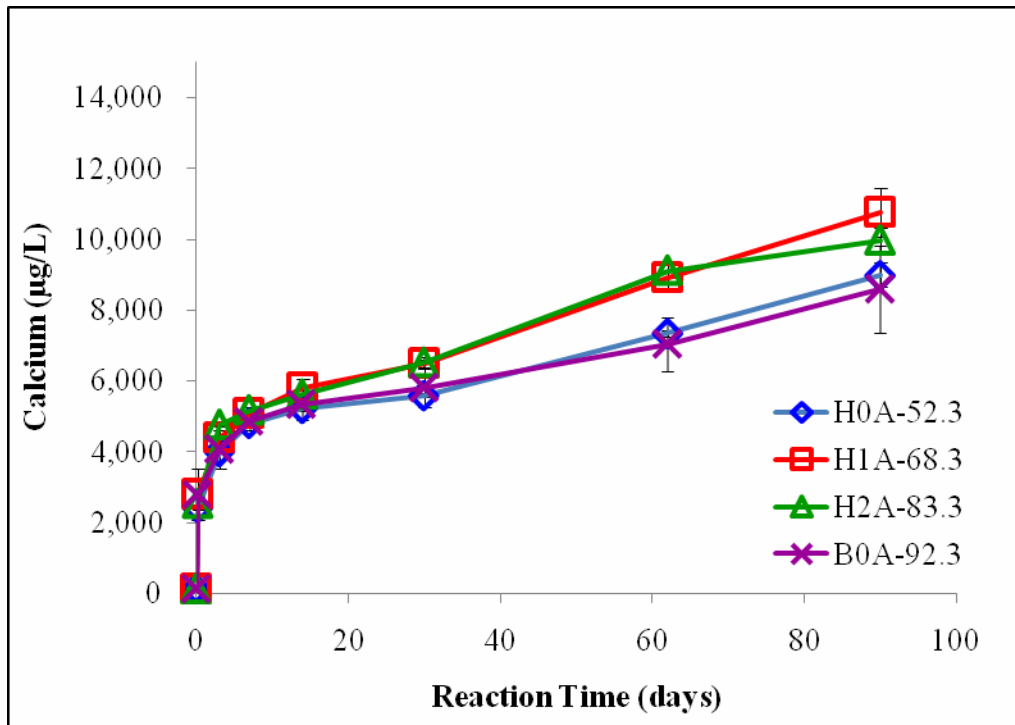


Figure 13. De-ionized water leaching, calcium in solution.

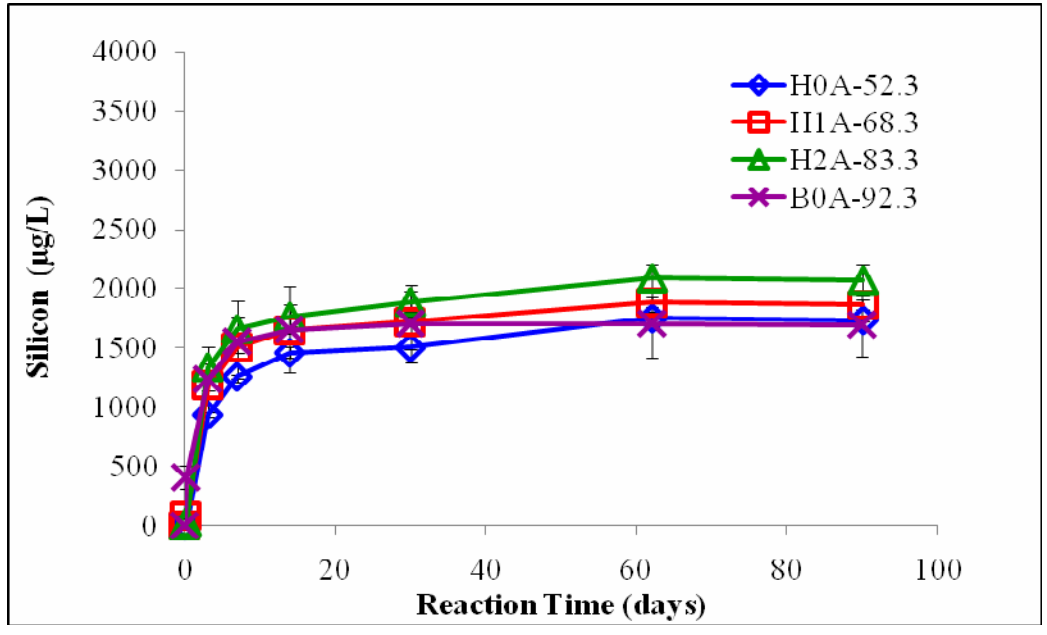


Figure 14. De-ionized water leaching, silicon in solution.

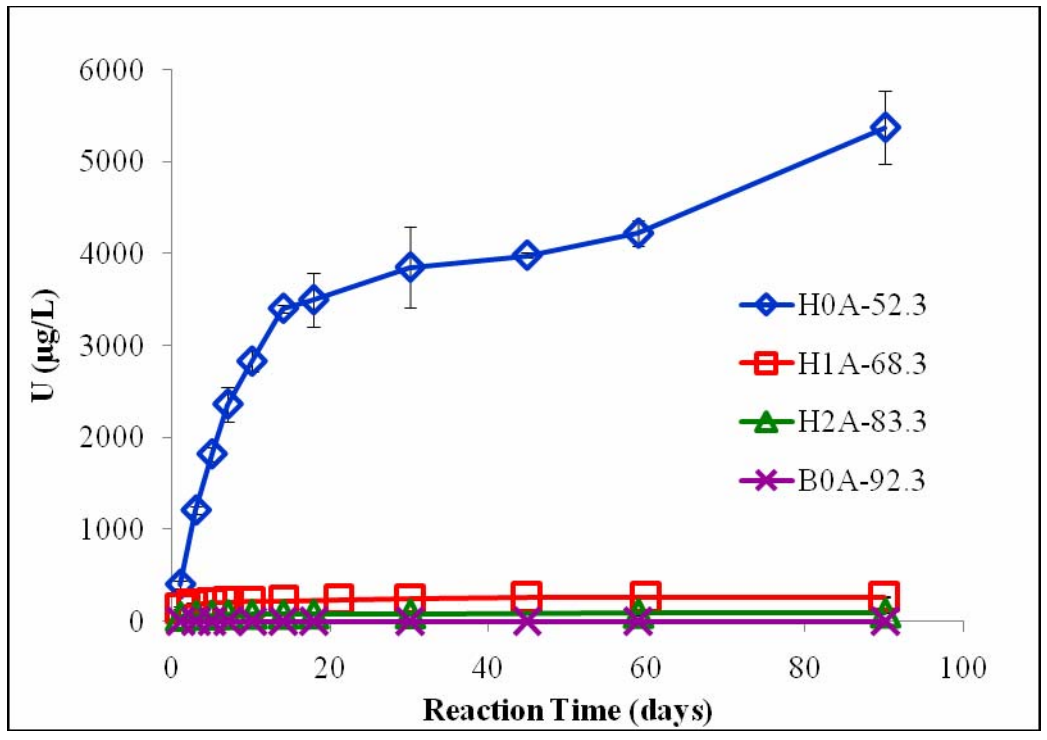


Figure 15 (Bi)carbonate leaching, uranium in solution.

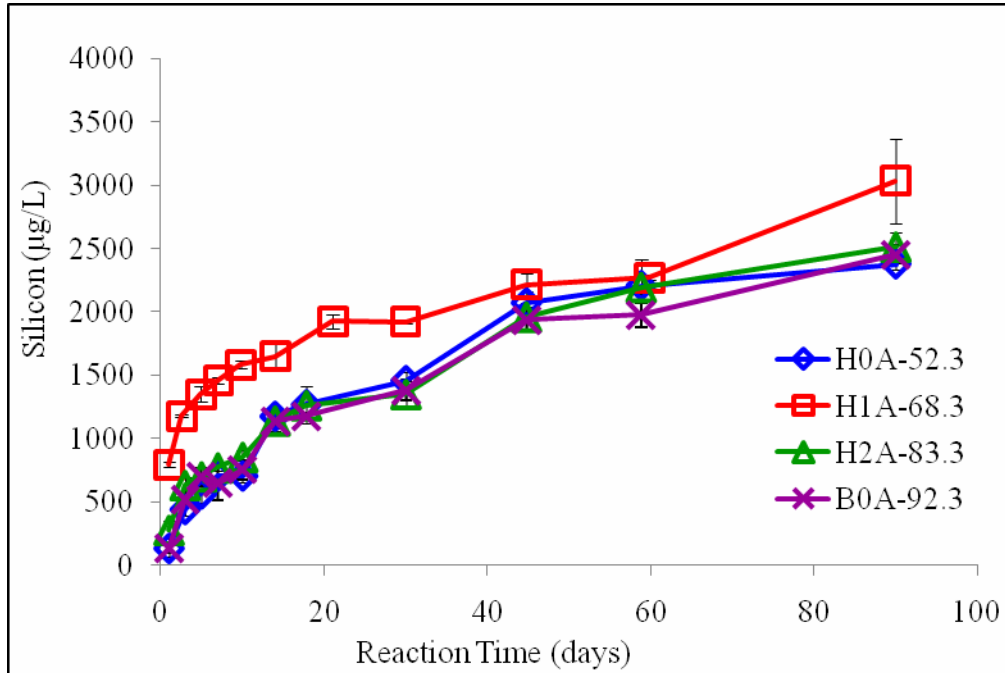


Figure 16. (Bi)carbonate leaching, silicon in solution.

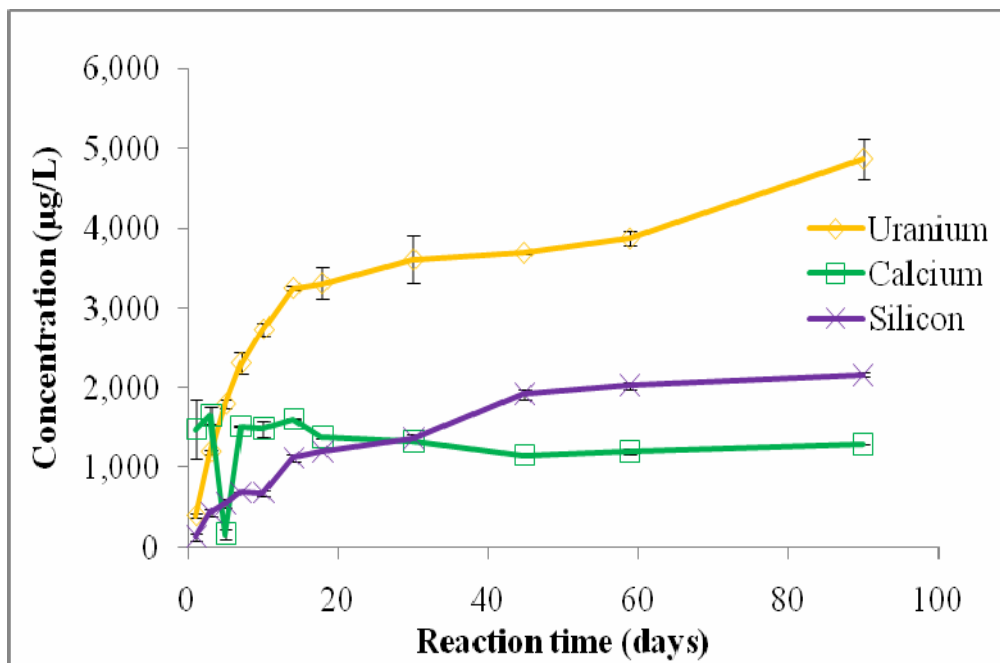


Figure 17. H0A-52.3 (bi)carbonate leaching, uranium, calcium, and silicon in solution.



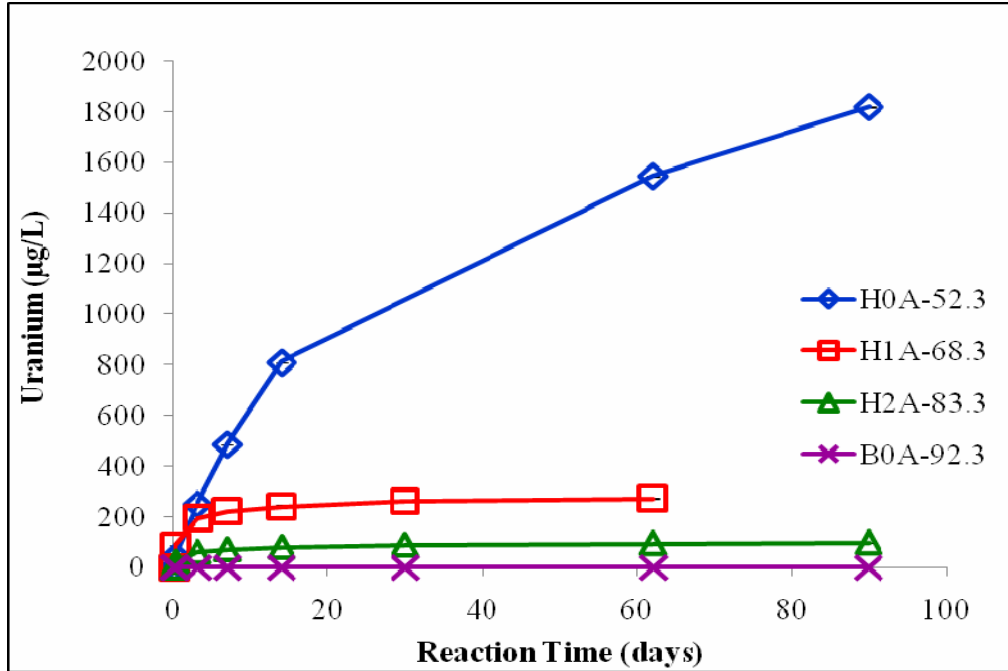


Figure 18. Synthetic groundwater leaching, uranium in solution.

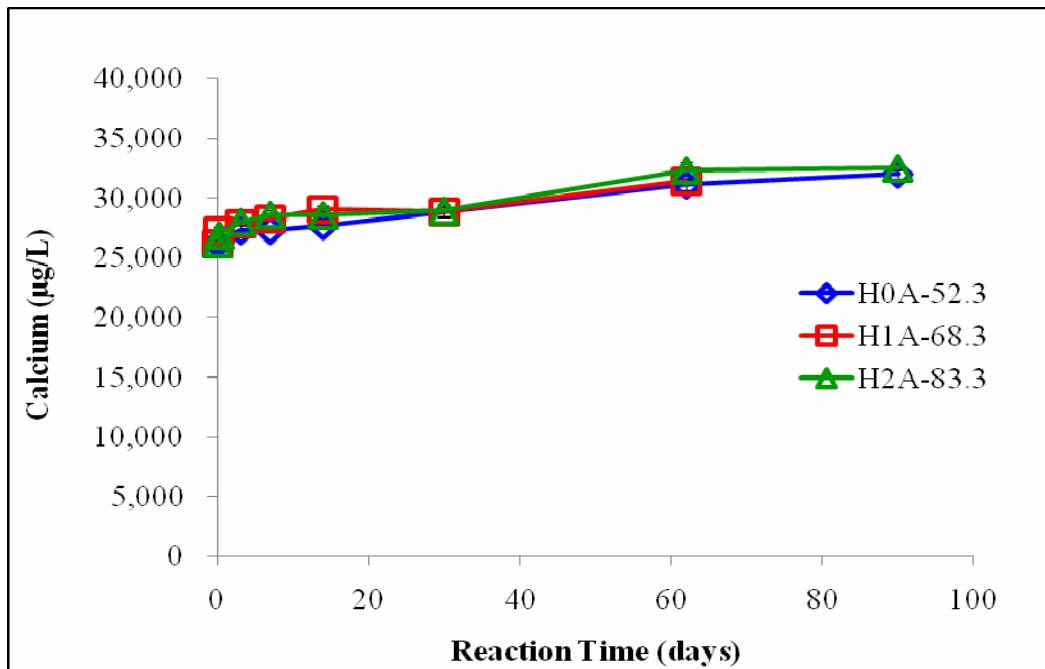


Figure 19. Synthetic groundwater leaching, calcium in solution.

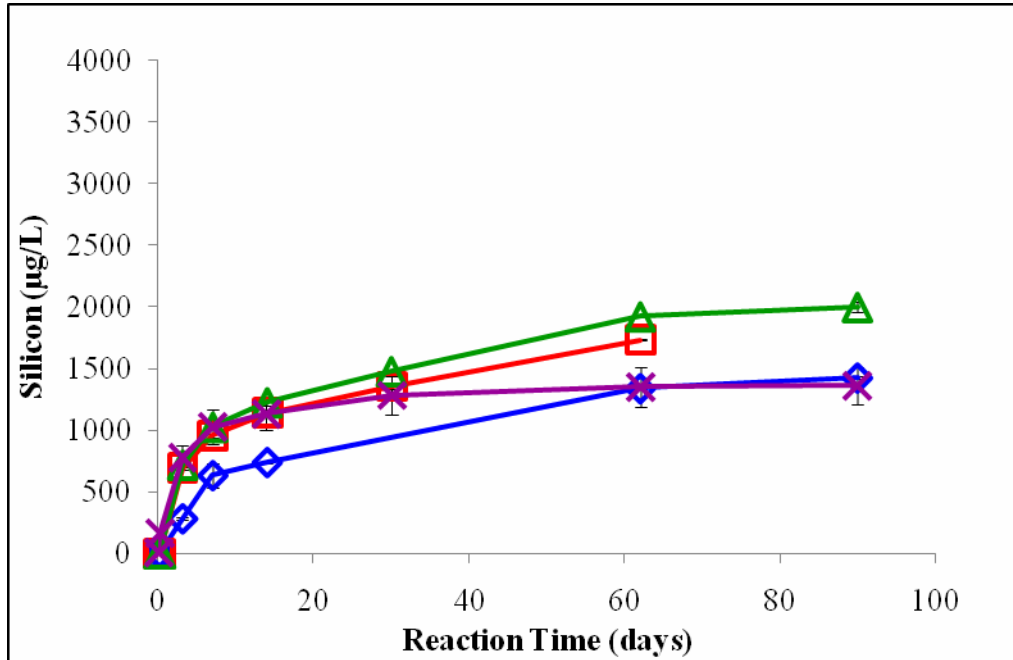


Figure 20. Synthetic groundwater leaching, silicon in solution.

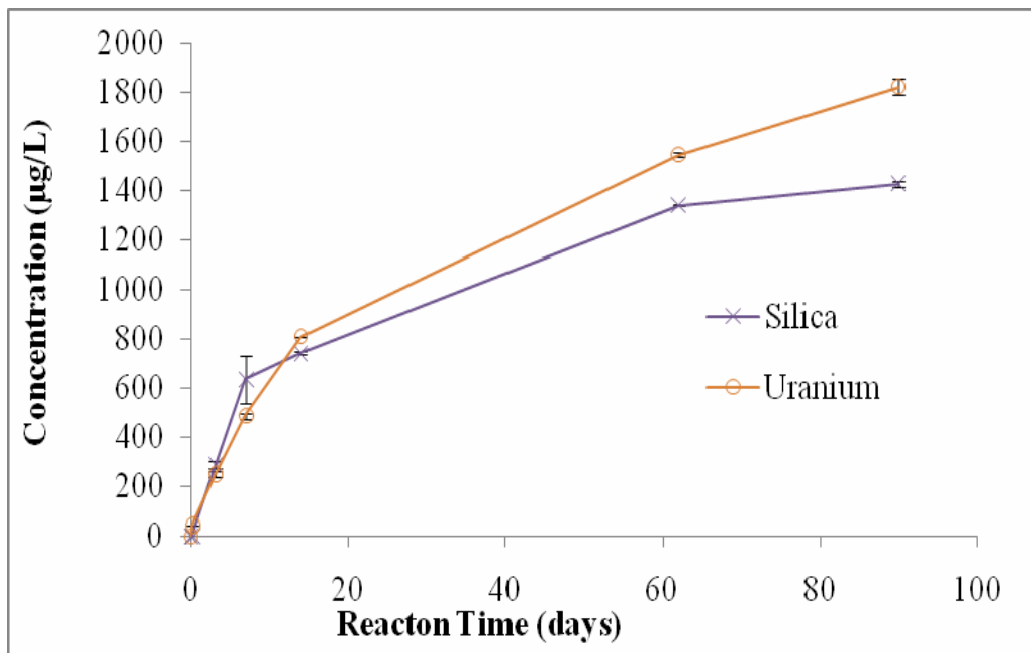


Figure 21. H0A-52.3 SGW leaching, silicon and uranium in solution.

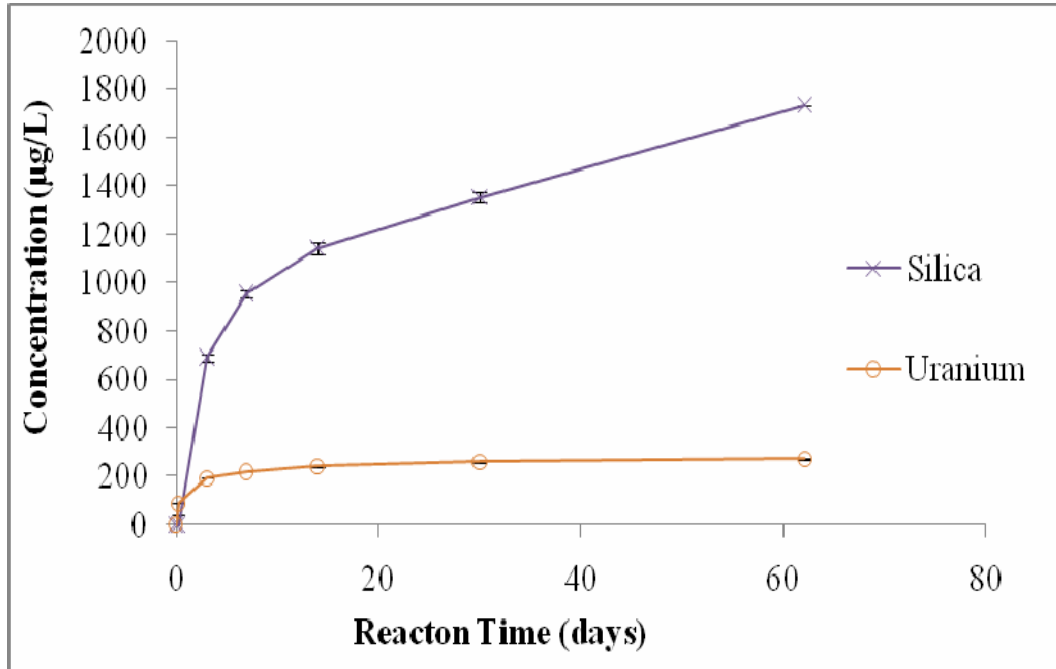


Figure 22. H1A-68.3 SGW leaching, silicon and uranium in solution.

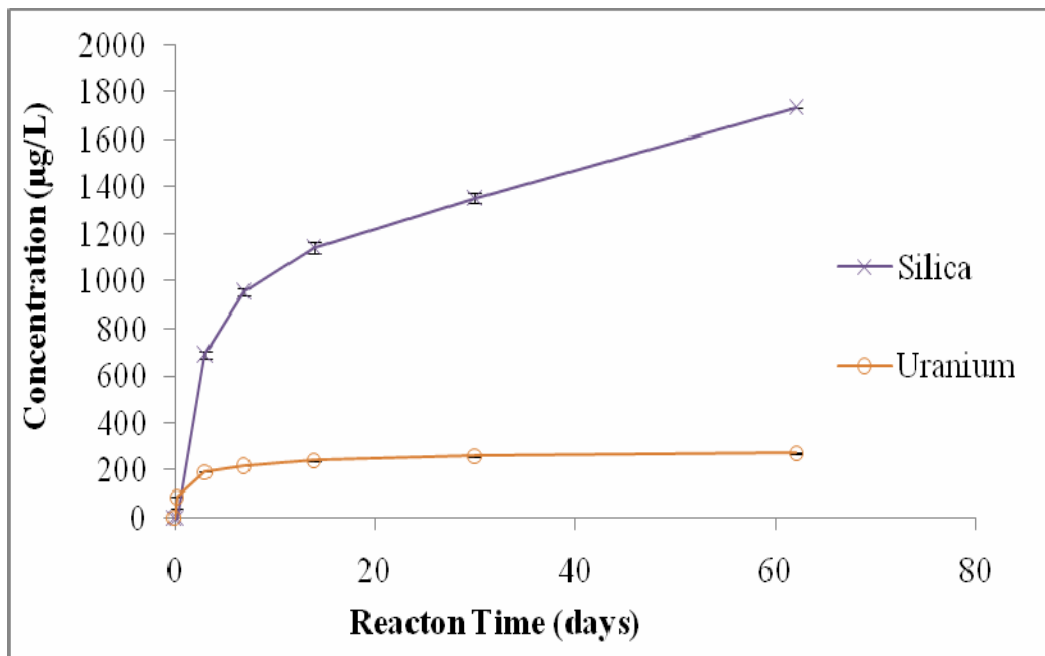


Figure 23. H2A-83.3 SGW leaching, silicon and uranium in solution

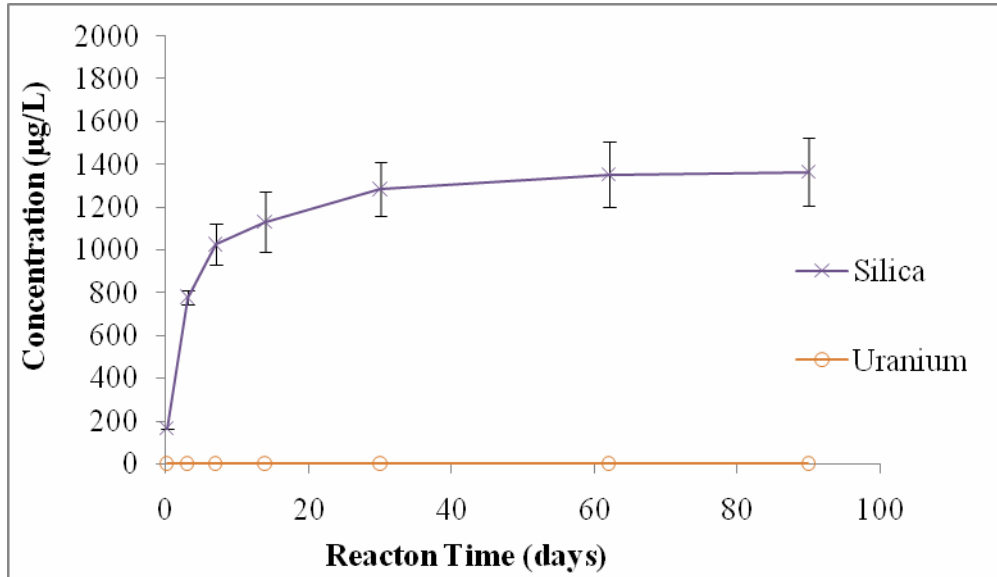


Figure 24. B0A-92.3 SGW leaching, silicon and uranium in solution.

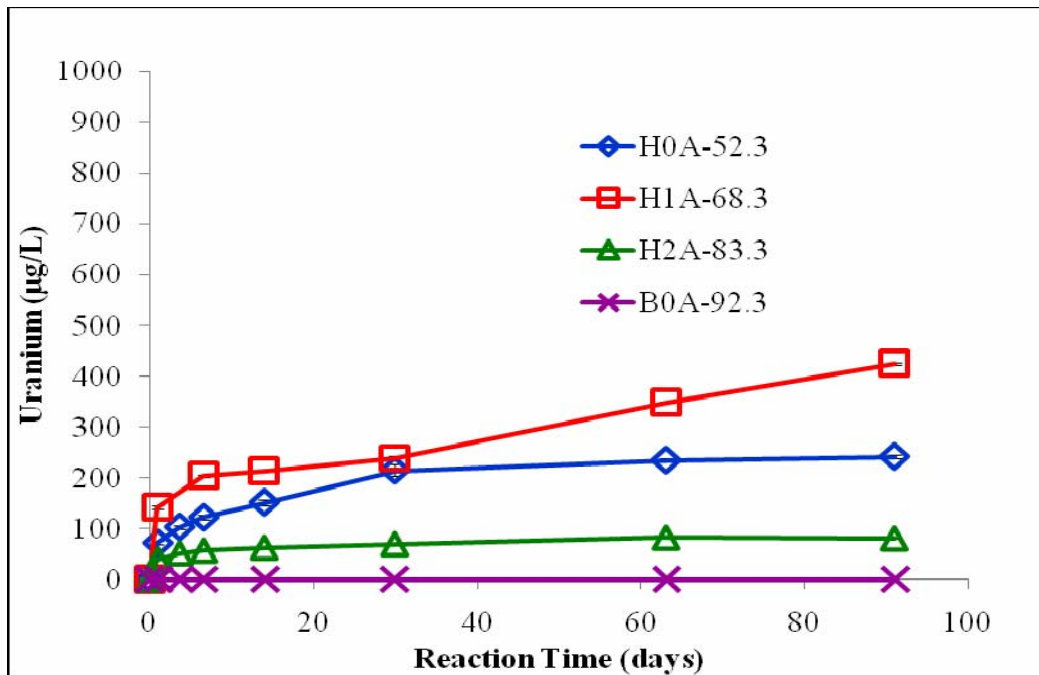


Figure 25. SGW+Na<sub>2</sub>SiO<sub>3</sub> leaching, uranium in solution.

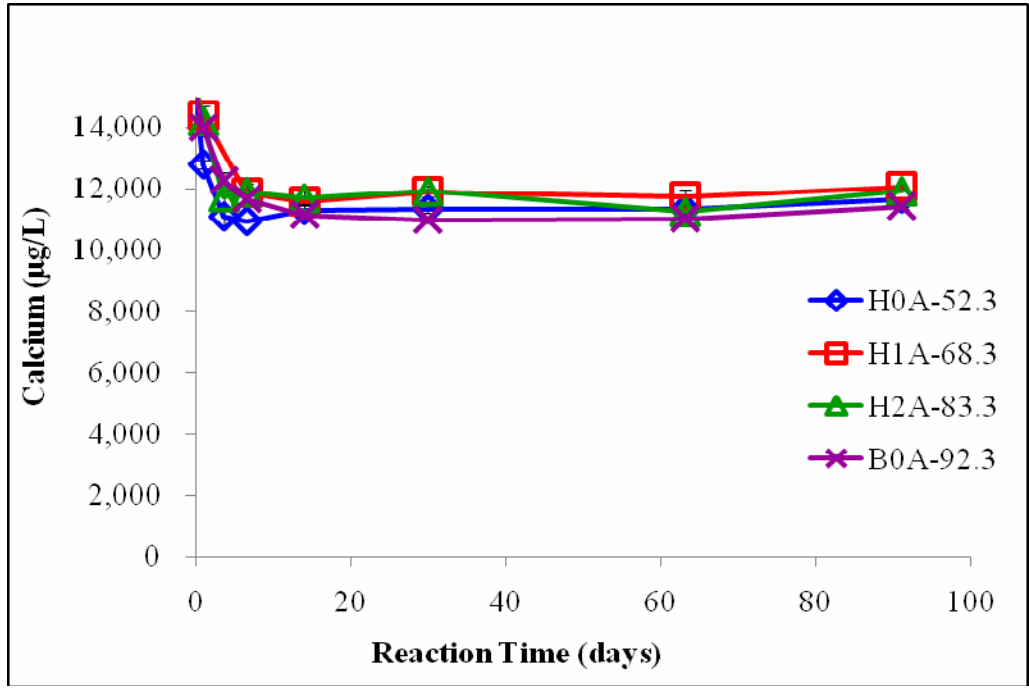


Figure 26. SGW+Na<sub>2</sub>SiO<sub>3</sub> leaching, calcium in solution.

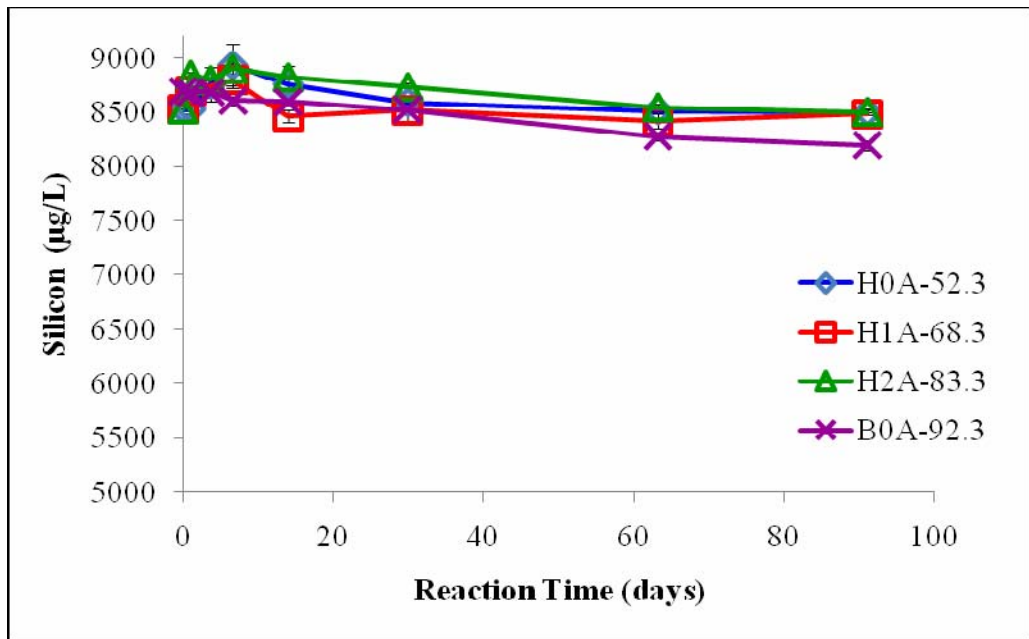


Figure 27. SGW+Na<sub>2</sub>SiO<sub>3</sub> leaching, silicon in solution.

## References

- Arai, Y., Marcus, M. K., Tamura, N., Davis, J. A. and Zachara, J. M., 2007. Spectroscopic evidence for uranium bearing precipitates in vadose zone sediments at the Hanford 300-area site. *Environmental Science & Technology* 41, 4633-4639.
- Brevick, C. H., Stroup, J. L. and Funk, J. W., 1997. Supporting document for the historical tank content estimate for U tank farm. Energy, U. S. D. o., Fluor Danile Northwest, Inc., HNF-SD-WM-ER-325, Rev. 1.
- Brown, C. F., Valenta, M. M., Serne, R. J., Bjornstad, B. N., Lanigan, D. C., Iovin, C., Clayton, R. E., Geiszler, K. N., Clayton, E. T., Kutnyakov, I. V., Baum, S. R., Lindberg, M. J. and Orr, R. D., 2007. Characterization of Direct Push Vadose Zone Sediments from the 241-U Single Shell Tank Farm. Pacific Northwest National Laboratory, Richland, Washington, PNNL-17163.
- Byrnes, M. E., 2001. Sampling and surveying radiological environments. CRC Press, Boca Raton, Florida
- Cantrell, K. J., Serne, R. J. and Last, G. V., 2003. Hanford Contaminant Distribution Coefficient Database and Users Guide. Energy, U. S. D. o., Pacific Northwest National Laboratory, PNNL-13895, Rev. 1.
- Catalano, J. G., McKinley, J. P., Zachara, J. M., Heald, S. M., Smith, S. C. and Brown, G. E., 2006. Changes in uranium speciation through a depth sequence of contaminated Hanford sediments. *Environmental Science & Technology* 40, 2517-2524.
- Crumpler, J. D., 2004. Site-Specific Single-Shell Tank Phase 1 RCRA Facility Investigation/Corrective Measures Study Work Plan Addendum for Waste Management Areas C, A-AX, and U. Energy, U. S. D. o., CH2M Hill Hanford Group, Inc., RPP-16608, Rev. 0.
- Deutsch, W. J., Cantrell, K. J. and Krupka, K. M., 2007. Contaminant Release Data Package for Residual Waste in Single-Shell Hanford Tanks. Energy, U. S. D. o., Pacific Northwest National Laboratory, PNNL-16748.
- Dong, W. M., Ball, W. P., Liu, C. X., Wang, Z. M., Stone, A. T., Bai, J. and Zachara, J. M., 2005. Influence of calcite and dissolved calcium on uranium(VI) sorption to a Hanford subsurface sediment. *Environmental Science & Technology* 39, 7949-7955.
- Drever, J. I., 2002. *The Geochemistry of Natural Waters*. Prentice-Hall, Upper Saddle River, New Jersey

- Field, J. G. and Jones, T. E., 2005. Tank Farm Vadose Zone Contamination Volume Estimates. Energy, D. o., CH2M HILL Hanford Group, Inc., RPP-23405, Rev. 2.
- Finch, R. and Murakami, T., 1999. Systematics and Paragenesis of Uranium Minerals. In: Burns, P. C. and Finch, R. (Ed), Uranium: Mineralogy, Geochemistry and the Environment, 38. The Mineralogical Society of America, Washington, D.C., pp. 679
- Gadelle, F., Wan, J. M. and Tokunaga, T. K., 2001. Removal of Uranium(VI) from contaminated sediments by surfactants. *Journal of Environmental Quality* 30, 470-478.
- Grenthe, I., Wanner, H., Forest, I. and Agency, O. N. E., 1992. Chemical thermodynamics of uranium. North-Holland, Elsevier Science Pub. Co., New York
- Hodges, F. N. and Chou, C. J., 2000a. Groundwater Quality Assessment for Waste Management Area U: First Determination. Pacific Northwest National Laboratory, Richland, Washington, PNNL-13282.
- Hodges, F. N. and Chou, C. J., 2000b. Groundwater Quality Assessment Plan for Single-Shell Tank Waste Management Area U at the Hanford Site. Pacific Northwest National Laboratory, PNNL-13185.
- Ilton, E. S., Qafoku, N. P., Liu, C. X., Moore, D. A. and Zachara, J. M., 2008. Advective removal of intraparticle uranium from contaminated vadose zone sediments, Hanford, US. *Environmental Science & Technology* 42, 1565-1571.
- Jenne, E. A., 1998. Adsorption of Metals by Geomedia. Academic Press, San Diego, CA
- Kaplan, D. I., Gervais, T. L. and Krupka, K. M., 1998. Uranium(VI) sorption to sediments under high pH and ionic strength conditions. *Radiochimica Acta* 80, 201-211.
- Kohler, M., Curtis, G. P., Meece, D. E. and Davis, J. A., 2004. Methods for estimating adsorbed uranium(VI) and distribution coefficients of contaminated sediments. *Environmental Science & Technology* 38, 240-247.
- Krupka, K. M., Serne, R. J. and Kaplan, D. I., 2004. Geochemical Data Package for the 2005 Hanford Integrated Disposal Facility Performance Assessment. Energy, U. S. D. o., Pacific Northwest National Laboratory, PNNL-13037, Rev. 2.
- Langmuir, D., 1997. Aqueous environmental geochemistry. Prentice-Hall, Upper Saddle River, New Jersey
- Last, G. V., Freeman, E. J., Cantrell, K. J., Fayer, M. J., Gee, G. W., Nichols, W. E., Bjornstad, B. N. and Horton, D. G., 2006. Vadose Zone Hydrogeology Data Package for Hanford Assessments. Energy, U. S. D. o., Pacific Northwest National Laboratory, PNNL-14702.

- Liu, C. X., Zachara, J. M., Qafoku, N. P. and Wang, Z. M., 2008. Scale-dependent desorption of uranium from contaminated subsurface sediments. *Water Resources Research* 44, 13.
- Liu, C. X., Zachara, J. M., Qafoku, O., McKinley, J. P., Heald, S. M. and Wang, Z. M., 2004. Dissolution of uranyl microprecipitates in subsurface sediments at Hanford site, USA. *Geochimica Et Cosmochimica Acta* 68, 4519-4537.
- Mason, C. F. V., Turney, W., Thomson, B. M., Lu, N., Longmire, P. A. and Chisholm-Brause, C. J., 1997. Carbonate leaching of uranium from contaminated soils. *Environmental Science & Technology* 31, 2707-2711.
- McKinley, J. P., Zachara, J. M., Wan, J., McCready, D. E. and Heald, S. M., 2007. Geochemical controls on contaminant uranium in vadose Hanford formation sediments at the 200 area and 300 area, Hanford Site, Washington. *Vadose Zone Journal* 6, 1004-1017.
- Qafoku, N. P., Zachara, J. M., Liu, C. X., Gassman, P. L., Qafoku, O. S. and Smith, S. C., 2005. Kinetic desorption and sorption of U(VI) during reactive transport in a contaminated Hanford sediment. *Environmental Science & Technology* 39, 3157-3165.
- Reidel, S. P. and Chamness, M. A., 2007. Geology Data Package for the Single-Shell Tank Waste Management Areas at the Hanford Site. Pacific Northwest National Laboratory, Richland, Washington, PNNL-15955.
- Singer, D. M., Zachara, J. M. and Brown, G. E., 2009. Uranium Speciation As a Function of Depth in Contaminated Hanford Sediments - A Micro-XRF, Micro-XRD, and Micro- And Bulk-XAFS Study. *Environmental Science & Technology* 43, 630-636.
- Smith, R. M., Hodges, F. N. and Williams, B. A., 2001. Groundwater Quality Assessment Plan for Single-Shell Tank Waste Management Area U. Pacific Northwest National Laboratory, Richland, Washington, PNNL-13612.
- Um, W., Serne, R. J. and Krupka, K. M., 2007. Surface complexation modeling of U(VI) sorption to hanford sediment with varying geochemical conditions. *Environmental Science & Technology* 41, 3587-3592.
- Um, W., Wang, Z. M., Serne, R. J., Williams, B. D., Brown, C. F., Dodge, C. J. and Francis, A. J., 2009. Uranium Phases in Contaminated Sediments below Hanford's U Tank Farm. *Environmental Science & Technology* 43, 4280-4286.
- Wan, J. M., Kim, Y. M., Tokunaga, T. K., Wang, Z. M., Dixit, S., Steefel, C. I., Saiz, E., Kunz, M. and Tamura, N., 2009. Spatially Resolved U(VI) Partitioning and Speciation: Implications for Plume Scale Behavior of Contaminant U in the Hanford Vadose Zone. *Environmental Science & Technology* 43, 2247-2253.



Wang, Z. M., Zachara, J. M., Yantasee, W., Gassman, P. L., Liu, C. X. and Joly, A. G., 2004. Cryogenic laser induced fluorescence characterization of U(VI) in hanford vadose zone pore waters. *Environmental Science & Technology* 38, 5591-5597.

Wellman, D. M., Zachara, J. M., Liu, C., Qafoku, N. P., Smith, S. C. and Forrester, S. W., 2008. Advective Desorption of Uranium(VI) from Contaminated Hanford Vadose Zone Sediments under Saturated and Unsaturated Conditions. *Vadose Zone Journal* 7, 1144-1159.

Wood, M. and Jones, T., 2003. Subsurface Conditions Description of The U Waste Management Areas. Energy, U. S. D. o., CH2M Hill Hanford Group, Inc., RPP-15808.

Zachara, J., Brown, C., Christensen, J., Davis, J., Dresel, E., Kelly, S., Liu, C., McKinley, J., Serne, J. and Um, W., 2007a. A Site-Wide Perspective on Uranium Geochemistry at the Hanford Site. Pacific Northwest National Laboratory, Richland, WA, PNNL-17031.

Zachara, J. M., Serne, J., Freshley, M., Mann, F., Anderson, F., Wood, M., Jones, T. and Myers, D., 2007b. Geochemical processes controlling migration of tank wastes in Hanford's vadose zone. *Vadose Zone Journal* 6, 985-1003.

## Figure Captions

1. Location map of the U tank farm at Hanford Site.
2. Tank U-104 uranium plume (Crumpler 2004).
3. XRD analysis of H0B-51.8 as compared to B0A-92.3
4. Particle size distribution of C5602 sediments.
5. Total uranium content by size fraction as determined by microwave digestion.
6. Uranium adsorption on B0A-91.8 in U-spiked SGW.
7. Adsorption reaction pH.
8. Adsorption reaction alkalinity.
9. B0A-91.8 adsorption isotherm at fourteen days.
10. Experimental data fit to linear form of Freundlich equation.
11. Experimental data fit to linear form of Langmuir equation.
12. De-ionized water leaching, uranium in solution.
13. De-ionized water leaching, calcium in solution.
14. De-ionized water leaching, silicon in solution.
15. (Bi)carbonate leaching, uranium in solution.
16. (Bi)carbonate leaching, silicon in solution.
17. H0A-52.3 (bi)carbonate leaching, uranium, calcium, and silica in solution.
18. Synthetic ground water leaching, uranium in solution.
19. Synthetic ground water leaching, calcium in solution.
20. Synthetic ground water leaching, silicon in solution.
21. H0A-52.3 SGW leaching, silicon and uranium in solution.

22. H1A-68.3 SGW leaching, silicon and uranium in solution.
23. H2A-83.3 SGW leaching, silicon and uranium in solution.
24. B0A-92.3 SGW leaching, silicon and uranium in solution.
25. SGW + Na<sub>2</sub>SiO<sub>3</sub> leaching, uranium in solution.
26. SGW + Na<sub>2</sub>SiO<sub>3</sub> leaching, calcium in solution.
27. SGW + Na<sub>2</sub>SiO<sub>3</sub> leaching, silicon in solution.

### **Table Captions**

1. Sediment samples from direct push hole C5602.
2. Chemical recipe for experimental solutions.
3. Synthetic ground water (SGW) uranium spike concentration.
4. Reactor Setup